## AD NUMBER

**ADB248332**

## NEW LIMITATION CHANGE

TO

**Approved for public release, distribution unlimited**

FROM

**Distribution authorized to U.S. Gov't. agencies only; Proprietary Info.; Oct 98. Other requests shall be referred to U.S. Army Medical Research and Material Command, 504 Scott St., Fort Detrick, MD 21702-5012.**

## AUTHORITY

**USAMRMC ltr, DTD 01 Jul 2003**

AD_____

GRANT NUMBER DAMD17-97-1-7030

TITLE: Magnetic Resonance Arterial Spin Tagging for Noninvasive Pharmacokinetic Analysis of Breast Cancer

PRINCIPAL INVESTIGATOR: Michael H. Buonocore, M.D.

CONTRACTING ORGANIZATION: University of California
Davis, California 95616-8671

REPORT DATE: October 1998

TYPE OF REPORT: Annual

PREPARED FOR: U.S. Army Medical Research and Materiel Command
Fort Detrick, Maryland 21702-5012

## NOTICE

USING GOVERNMENT DRAWINGS, SPECIFICATIONS, OR OTHER DATA INCLUDED IN THIS DOCUMENT FOR ANY PURPOSE OTHER THAN GOVERNMENT PROCUREMENT DOES NOT IN ANY WAY OBLIGATE THE U.S. GOVERNMENT. THE FACT THAT THE GOVERNMENT FORMULATED OR SUPPLIED THE DRAWINGS, SPECIFICATIONS, OR OTHER DATA DOES NOT LICENSE THE HOLDER OR ANY OTHER PERSON OR CORPORATION; OR CONVEY ANY RIGHTS OR PERMISSION TO MANUFACTURE, USE, OR SELL ANY PATENTED INVENTION THAT MAY RELATE TO THEM.

## LIMITED RIGHTS LEGEND

Award Number: DAMD17-97-1-7030
Organization: University of California
Location of Limited Rights Data (Pages):

Those portions of the technical data contained in this report marked as limited rights data shall not, without the written permission of the above contractor, be (a) released or disclosed outside the government, (b) used by the Government for manufacture or, in the case of computer software documentation, for preparing the same or similar computer software, or (c) used by a party other than the Government, except that the Government may release or disclose technical data to persons outside the Government, or permit the use of technical data by such persons, if (i) such release, disclosure, or use is necessary for emergency repair or overhaul or (ii) is a release or disclosure of technical data (other than detailed manufacturing or process data) to, or use of such data by, a foreign government that is in the interest of the Government and is required for evaluational or informational purposes, provided in either case that such release, disclosure or use is made subject to a prohibition that the person to whom the data is released or disclosed may not further use, release or disclose such data, and the contractor or subcontractor or subcontractor asserting the restriction is notified of such release, disclosure or use. This legend, together with the indications of the portions of this data which are subject to such limitations, shall be included on any reproduction hereof which includes any part of the portions subject to such limitations.

THIS TECHNICAL REPORT HAS BEEN REVIEWED AND IS APPROVED FOR PUBLICATION.

Patricia A. Anderson 10/4/99

# REPORT DOCUMENTATION PAGE

*Form Approved*
*OMB No. 0704-0188*



| 1. AGENCY USE ONLY *(Leave blank)* | 2. REPORT DATE | 3. REPORT TYPE AND DATES COVERED |
|---|---|---|
| | October 1998 | Annual (30 Sep 97 - 29 Sep 98) |

**4. TITLE AND SUBTITLE**
Magnetic Resonance Arterial Spin Tagging for Noninvasive Pharmacokinetic Analysis of Breast Cancer

**5. FUNDING NUMBERS**
DAMD17-97-1-7030

**6. AUTHOR(S)**
Buonocore, Michael H., M.D.

**7. PERFORMING ORGANIZATION NAME(S) AND ADDRESS(ES)**
University of California
Davis, California 95616-8671

**8. PERFORMING ORGANIZATION REPORT NUMBER**

**9. SPONSORING / MONITORING AGENCY NAME(S) AND ADDRESS(ES)**
U.S. Army Medical Research and Materiel Command
Fort Detrick, Maryland 21702-5012

**10. SPONSORING / MONITORING AGENCY REPORT NUMBER**

**11. SUPPLEMENTARY NOTES**

**12a. DISTRIBUTION / AVAILABILITY STATEMENT**
Distribution authorized to U.S. Government agencies only (proprietary information, Oct 98). Other requests for this document shall be referred to U.S. Army Medical Research and Materiel Command, 504 Scott Street, Fort Detrick, Maryland 21702-5012.

**12b. DISTRIBUTION CODE**

**13. ABSTRACT** *(Maximum 200 words)*

This project is designed to develop and evaluate arterial spin tagging techniques for the non-invasive measurement of breast tissue perfusion. The long term goal is to show that arterial spin tagging can provide comparable tissue information as that currently obtained using dynamic first-pass contrast-enhanced imaging. To date, the research effort has focused on the pulse sequence, protocol and image processing software needed for analysis and visualization of the anatomic, functional, and dynamic breast images. Specific tests and analyses of the sequence have been performed to understand and correct for driven equilibrium effects, and for inversion and excitation slice profile mismatch. Software development includes methods for estimating, at each pixel, the $T_1$, the perfusion (as defined by $f/\lambda$), and standard errors, and from these compute a "suspicion index" that the tissue is abnormal. Algorithms for image registration and image display have been developed to allow direct comparison of high resolution $T_1$, fast spin echo $T_2$ and proton density, perfusion, and contrast enhanced images. The research effort provides crucial software for acquisition and definitive review of the images, and automation for detailed and thorough statistical analysis of the very large data sets that are obtained.

| 14. SUBJECT TERMS | | 15. NUMBER OF PAGES |
|---|---|---|
| Breast Cancer | Magnetic resonance imaging, Detection, Tissue perfusion, Arterial spin tagging, pharmacokinetic analysis | 51 |
| | | 16. PRICE CODE |

| 17. SECURITY CLASSIFICATION OF REPORT | 18. SECURITY CLASSIFICATION OF THIS PAGE | 19. SECURITY CLASSIFICATION OF ABSTRACT | 20. LIMITATION OF ABSTRACT |
|---|---|---|---|
| Unclassified | Unclassified | Unclassified | Limited |

## FOREWORD

Opinions, interpretations, conclusions and recommendations are those of the author and are not necessarily endorsed by the U.S. Army.

____ Where copyrighted material is quoted, permission has been obtained to use such material.

____ Where material from documents designated for limited distribution is quoted, permission has been obtained to use the material.

MHB Citations of commercial organizations and trade names in this report do not constitute an official Department of Army endorsement or approval of the products or services of these organizations.

____ In conducting research using animals, the investigator(s) adhered to the "Guide for the Care and Use of Laboratory Animals," prepared by the Committee on Care and use of Laboratory Animals of the Institute of Laboratory Resources, national Research Council (NIH Publication No. 86-23, Revised 1985).

MHB For the protection of human subjects, the investigator(s) adhered to policies of applicable Federal Law 45 CFR 46.

____ In conducting research utilizing recombinant DNA technology, the investigator(s) adhered to current guidelines promulgated by the National Institutes of Health.

____ In the conduct of research utilizing recombinant DNA, the investigator(s) adhered to the NIH Guidelines for Research Involving Recombinant DNA Molecules.

____ In the conduct of research involving hazardous organisms, the investigator(s) adhered to the CDC-NIH Guide for Biosafety in Microbiological and Biomedical Laboratories.

Michael H Bunnone 10/28/98

PI - Signature Date

# (4) TABLE OF CONTENTS

## (5) INTRODUCTION

**Subject:** This study concerns the development of MRI arterial spin tagging to non-invasively measure breast tissue perfusion. The project will test whether the tagging technique is a low cost and more reliable alternative to dynamic first-pass contrast-enhanced imaging, giving possibilities for use in specific clinical settings, as well as in screening. MR dynamic first-pass contrast-enhanced imaging has shown that malignant and benign breast lesions can be distinguished. However, it may have limited importance in clinical breast diagnosis due to significant false-negatives and false-positives. Also, dynamic contrast enhancement cannot be used in screening, even within defined high-risk sub-populations such as patients with dense breasts, due to the high cost of contrast material and administration. The arterial spin tagging technique was developed to measure tissue perfusion parameters without the use of contrast, and has been successfully demonstrated in brain and kidney. The spin tagging technique may provide more sensitive and specific assessment of these parameters, at higher spatial resolutions, by virtue of its ability to acquire repeated measurement of flow sensitive data to improve signal to noise ratio (SNR). Dynamic first-pass contrast-enhanced imaging has a limited data acquisition time and thus a limited resolution and SNR.

**Purpose:** The purpose (long-term goal) of the project is to develop MRI arterial spin tagging as a low cost and more reliable alternative to first-pass contrast-enhanced imaging. We will test the hypothesis that arterial spin tagging provides accurate and precise discrimination between normal tissue, benign and malignant lesions, when differences in perfusion and $T_1$ exist. Lesions will have been previously detected by clinically accepted diagnostic imaging procedures, and by biopsy. Statistical analysis will be performed to access the correspondence between arterial spin-tagging and biopsy, and to establish the relative value of spin tagging compared to first-pass contrast-enhanced MRI. We hope to establish that, relative to using first-pass contrast-enhanced imaging, false positives and negatives are reduced using arterial spin tagging by virtue of increased image signal-to-noise ratio (SNR), higher spatial resolution, and the unique ability to obtain estimates of macromolecular bound fluid fractions.

**Scope:** The effort on the project is mainly limited to the technical aspects of development of a new methodology. However, the project also includes a rigorous performance comparison with the current gold-standard methodology. The specific aims are to (1) refine arterial spin tagging pulse sequences and imaging protocols, (2) develop automated data analysis software for measurement of breast tissue parameters, and (3) compare the technique to first-pass contrast-enhanced MRI and biopsy. The technique will be evaluated in sixty patients, with roughly equal numbers of benign and malignant lesions. Multi-component differential equation models of magnetization distribution within breast tissue will be used to estimate perfusion and $T_1$, from which regions suspicious for malignant disease will be identified. While sub-population screening is a critical potential application, it is premature to propose a study to evaluate the technique for specific sub-population screening, before it's capability for detection and discrimination of previously detected lesions is established.

**Background:** Studies have shown that dynamic first-pass contrast-enhanced magnetic MRI discriminates malignant from many types of benign breast disease. This technique detects malignant disease by measuring tissue fluid distribution parameters, which are derived from the rate of rise of MRI signal intensity. The rate of decrease of signal intensity, after the peak signal is reached, is also believed to be related to malignancy, based on the idea that the vasculature of

malignant tissues possesses a high degree of arteriovenous shunting causing more rapid elimination of contrast agent. Unfortunately, this technique may have limited importance due to significant false-negatives and false-positives. Further development and refinement is required, but major improvements are unlikely given the limited data acquisition time inherent to first-pass techniques. In particular, the first-pass techniques cannot provide, with high temporal resolution, high spatial resolution required to reveal morphological details that can reduce false positives. Arterial spin tagging has been developed for measuring tissue parameters without the use of contrast, and has been successfully demonstrated in brain and kidney. Spin tagging measures absolute blood perfusion (cc/min/g tissue), longitudinal relaxation time ($T_1$) of the tissue water, and possibly macromolecular bound fluid fractions. Spin tagging can provide more sensitive and specific assessment of tissue parameters, at higher spatial resolution, using the ability to build up signal to noise over reasonable scan times to investigate tissue parameters. It is not limited to data collection during a first pass.

Previous studies have confirmed that first-pass enhancement of carcinomas by Gd-DTPA are often (but not always) more intense and faster compared to normal parenchyma or benign breast disease [1,2,3,4,5,6,7,8]. Enhancement is attributed to tumor-induced angiogenesis resulting in increased vascularity within the malignant tumor [9,10,11] which often also develops anastomoses and shunts. Due to greater tissue uptake, carcinomas enhance maximally within 1.5 to 2 minutes of contrast injection and then, due to accumulation in extracellular fluid, tend to maintain the enhancement for several minutes. Kaiser [12] postulated that false positive benign lesions may be distinguished by the behavior of signal enhancement after the peak occurs, i.e., during the elimination phase [13]. Malignant lesions have greater degrees of A/V shunting, and hence more rapid elimination of contrast and more rapid return to non-enhanced signal levels. Due to the importance of the time course of signal enhancement in these criteria, pharmacokinetic analysis [8,14,15] has been clinically important. Motion correction [16] and image subtraction [17] have been important for reliable temporal processing. However, the importance of morphology is regarded by many researchers as equally or more important than temporal profiles, and some have emphasized high spatial resolution, not temporal resolution, in discrimination of tumors [18,19 page 595]. Overall, inconsistent reports and general overlap of benign and malignant temporal profiles precludes the role of MRI as an "imaging biopsy" [19,20].

Techniques for non-invasive, spatially resolved MRI perfusion measurement have been developed based on magnetic labeling of arterial water [21,22] (i.e. arterial spin-tagging), and tested in both animals and humans [23,24,25,26]. Mathematical models of the magnetization distribution are used to relate changing signal intensity to tissue perfusion (flow of magnetization into tissue), magnetization of free fluid, magnetization of fluid bound to macromolecules, and fluid exchange rates between these compartments [23,27]. Tagged spins will not accumulate significantly in tissues as does contrast agent, and therefore do not obtain precisely the same measurements as contrast-enhanced scans. However, arterial spin tagging will measure macromolecular bound fluid fraction, that is affected by extracellular fluid fraction, and can be adapted to measurement of fluid elimination.

## (6) BODY

*Overview*

This section details the experimental methods, results and discussion in relation to the Statement of Work outlined in the proposal. The first subsection provides brief paragraphs of the accomplishments in relation to the Statement of Work. Detailed discussion of these accomplishments is provided in the second subsection. There are two main contributions of the work. The first is the discovery of a multitude of unrecognized sources of $T_1$ estimate errors, the recognition of the profound sensitivity of perfusion measurements to $T_1$ estimate errors, and the development of robust pulse sequences and analysis methods to derive accurate $T_1$ estimates with inherently noisy and confounded signal data. The second is the development of the software program, BrView, to allow rapid review, quantitative analysis, and assessment of the multitude of different breast images and timeseries data that is obtained in each patient study.

*Summary of accomplishments in relation to Statement of Work*

Technical objective 1

*Task 1*: Months 1-6: Implementation and testing of magnetization transfer pulses for both arterial tagging and first-pass contrast enhanced sequences.

Magnetization transfer pulses have not been implemented yet. Mainly, this delay was due to the fact that the MRI system at UC Davis Medical Center is scheduled to be upgraded to the new Horizon LX system soon, and we opted to defer this pulse sequence development until we were using this new LX software platform. There have been multiple delays, but this upgrade is scheduled to occur by January 1999. The existing pulse sequence will be converted from the 5.4 OS platform to the LX2 platform (a substantial change), and the magnetization transfer pulses will be implemented also.

Because of concerns regarding the ultimate utility of the magnetization transfer technique, we have decided that implementation and testing of arterial spin-tagging sequence based on echo planar imaging (EPI) data acquisition is a higher priority. EPI based spin-tagging technique can theoretically improve the accuracy of the $T_1$ estimation, which we have studied and worked with extensively (see below). The major problem with magnetization transfer is that it represents a perturbation on an already small signal. Therefore, whether we will observe a magnetization transfer effect is questionable. Nevertheless, it will be implemented as part of the project.

*Task 2*: Months 1-9: Implementation and testing of interleaved high-resolution imaging technique, for both arterial tagging and first-pass contrast enhanced sequences.

An interleaved arterial spin-tagging technique, that allows high resolution (e.g. 256 x 256 or more) has been implemented and tested. We also implemented a rectangular data acquisition technique, which acquires data sets that have different numbers of points along the frequency and phase encode direction. The 256 x 240 interleaved acquisition provides the best spatial versus temporal resolution tradeoff, and has been used for all of our recent studies.

*Task 3*: Months 1-9: Analysis of spin tagging sequence to understand causes of existing baseline offsets, effects of inversion slice transition profiles, and effects of RF flip angle profile on the measurements, with implementation and testing pulse sequence modifications to minimize these imperfections.

Matching of inversion and excitation slice profiles was greatly improved by using customized RF pulses designed with the Shinnar-Le Roux (SLR) algorithm. The new data processing technique (based on a semi-log linear regression of inversion time (*TI*) dependent signal) significantly reduced the previously reported problem in measuring the longitudinal relaxation time ($T_1$) caused by baseline offsets, and by the uncertainty in the effective inversion time. The optimal RF flip angle for spin excitation during spatial encoding was found to be 10 degrees, based on experiments over a range of flip angles.

Technical objective 2

*Task 4*: Months 3-15: Software for automatic estimation and error analysis of perfusion, tissue water longitudinal relaxation time, and extracellular fluid volume fraction from mathematical models and user-defined ROIs from spin tagging timeseries. Implementation of pharmacokinetic model calculations and error analysis for first-pass contrast enhanced imaging.

A software program (BrView) has been written in C, X Window System, and Motif, and implemented on an SGI O2 computer (paid for by grant funds) for analyzing and visualizing the MR images and timeseries. Much effort has been expended on developing the capability to easily review all of the images taken in each study, and cross-reference pixel locations. Much more effort than anticipated has been expended in the development of a robust technique for identifying so-called "suspicious regions" based on the $T_1$ and perfusion measurements. The measurement of $T_1$, upon which the perfusion measurement entirely depends, is based on a semi-log linear regression technique developed by the investigators. The $T_1$, perfusion ($f/\lambda$) and standard errors of these quantities are estimated automatically using this robust technique. The so-called feature images display these quantities in color and grayscale. These quantities are used to calculate a "suspicion index" for each pixel, and thereby identify regions of breast tissue suspicious for malignancy.

The implementation of the pharmacokinetic model calculations and error analysis for first-pass contrast enhanced imaging has not been completed. Thus far, the software allows the user to click on the reference image of the dynamic study, to display the time profile of the signal at that pixel. The implementation of the pharmacokinetic model is currently a major focus of the current effort.

*Task 5*: Months 3-15: Software for registration (including implementation and testing of motion correction and physiological noise reduction algorithms) and overlay of images from high resolution $T_1$ weighted, spin-tagging, and contrast enhanced studies.

Using the BrView software program, image pixels containing high values of perfusion ($f/\lambda$), and moderate to high values of $T_1$, and low standard errors, are identified as suspicious, and assigned a "suspicion index" based on finding similar abnormal values at spatially adjacent pixels. Suspicious pixels can be overlaid on the high-resolution $T_1$ and $T_2$ clinical images by color mapping, and simultaneously presented with the first-pass contrast enhanced timeseries at these pixels. This provides the user with a comprehensive anatomical and functional view of the suspicious regions, and facilitates making a decision regarding the malignant nature of the lesion. Finally, a motion artifact estimation and correction algorithm has been developed and implemented in a separate software program.

Technical objective 3

*Task 6*: Months 9-24: 60 patients with malignant and benign breast lesions will be imaged using $T_1$ weighted, first-pass contrast enhanced, and arterial spin tagging MRI pulse sequences.

We have recruited only two subject studies for both first-pass contrast enhanced and arterial spin tagging MRI pulse sequences. Now that the software development is substantially completed, we are trying to improve the rate at which patients are recruited into the study. It is likely that the patient studies will extend into the third year of the proposal. We are currently discussing with physicians at a local Kaiser Hospital for recruitment of additional patients. Appropriate documentation will be submitted for approvals upon reaching a firm agreement.

***Detailed description of the accomplishments***

Background to theory of arterial spin tagging

This background material is taken from the literature, and represents the starting point for the project. In the so-called "on-slice" spin tagging technique that we implemented, spins in a slab of tissue are inverted first using a RF pulse. The thickness of the slab can be controlled by the strength of the slab selective gradient (normally a Z gradient). Then the levels of recovery to equilibrium are measured at different times (**Figure 1**). The rate of recovery (i.e. the effective $T_1$) can be estimated from the recovery curve. In the research protocol, 3mm slices are imaged

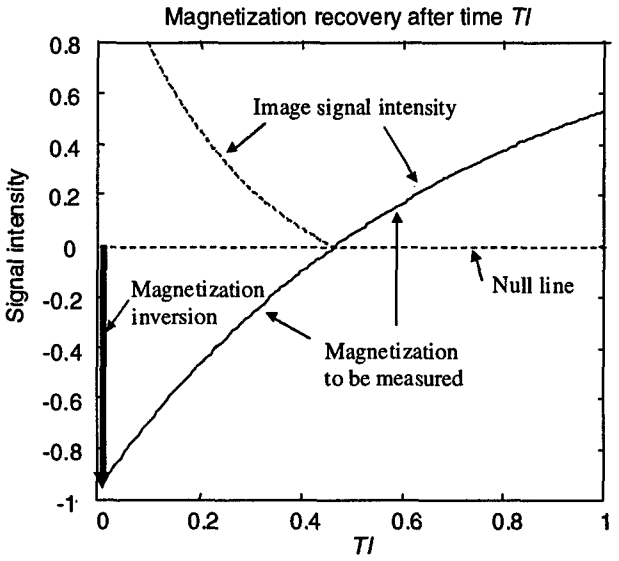


Figure 1. After the Magnetization is inverted, it recovers towards thermal equilibrium position according to characteristic relaxation time $T_1$. The signal intensity along a typical magnetization recovery curve is shown. The image displays the magnitude of the magnetization. The rate of recovery can be determined from images acquired at different times of the recovery curve represented by *TI*. *TI* is a point in time at which an zero k-space line is acquired.

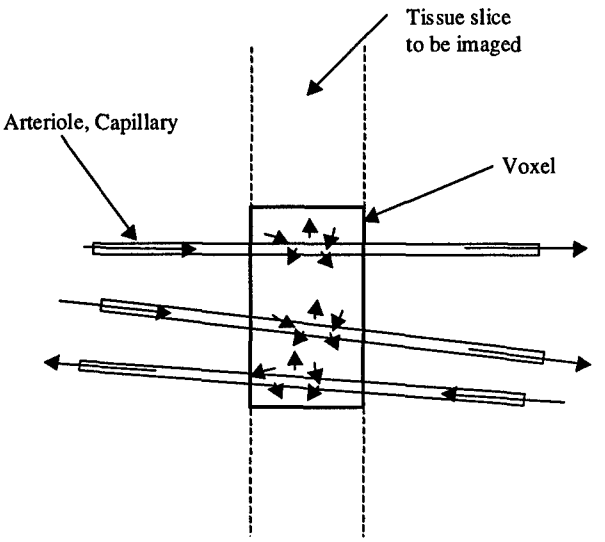


Figure 2. A voxel within the imaged slice is identified. Arterioles and capillaries pass through the voxel resulting in net blood flow (indicated by long arrows) and replacement of tissue water. Blood water (indicated by short arrows) exchanges readily with the extracellular fluid.

sequentially (one at a time). The goal is to measure capillary blood perfusion, which is defined as the net amount of arterial blood per second entering a gram of breast tissue. This definition can be extended to a per unit volume (voxel) measurement, i.e., the net amount of arterial blood per second entering a voxel of breast

tissue. Therefore, perfusion represents the directed microscopic flow within a voxel. In breast tissue, blood vessels, which are basically composed of capillaries, are very small. Blood flow is very slow in these vessels. Water molecules can move easily between the vessels and their surroundings (**Figure 2**). A two-component model is used to approximate the activity of the water molecules. In this model, water molecules in blood vessels entering a slice of breast tissue mix thoroughly with water molecules outside the vessels before they leave the slice. For this two-component model, the Bloch Equation for the breast tissue water magnetization at the slice of tissue investigated can be written as [23]

$$\frac{dM(t)}{dt} = \frac{M_0 - M(t)}{T_1} - k_{for}\, M_m(t) + k_{rev}\, M_m(t) + f\, M_a(t) - f\left(\frac{M(t)}{\lambda}\right) \qquad (1.1)$$

where, $M(t)$ = the longitudinal water magnetization of a voxel of breast tissue at time $t$, $M_0$ = the value of $M(t)$ under fully relaxed conditions, $T_1$ = the spin-lattice relaxation time constant of the breast tissue, $M_m(t)$ = the longitudinal magnetization of macromolecules in a voxel of tissue, $k_{for}$, $k_{rev}$ = the magnetization transfer rate constants from water to macromolecules and vice versa, $M_a$ = the longitudinal water magnetization per ml of arterial blood entering a voxel from outside of the slice investigated, $f$ = perfusion in ml of arterial blood per second in a voxel, and $\lambda$ = the ratio of water content between breast tissue overall and the arterial blood within it.

To simplify Eq.(1.1), we assume that the magnetization transfer contributions are negligible, specifically,

$$\left|(k_{rev} - k_{for})\, M_m(t)\right| << \left|\frac{M_0 - M(t)}{T_1} + f\, M_a(t) - f\left(\frac{M(t)}{\lambda}\right)\right|$$

Then Eq. (1.1) can be simplified to

$$\frac{dM(t)}{dt} = \frac{M_0 - M(t)}{T_1} + f\, M_a(t) - f\left(\frac{M(t)}{\lambda}\right) \qquad (1.2)$$

Eq. (1.1) will be utilized without this approximation when magnetization transfer is implemented. Parameters $T_1$ and $f/\lambda$ in Eq. (1.2) can be estimated from two spin tagging conditions. In the so-called "Selective Tagging Condition", all spins within the slice of breast tissue being imaged are inverted, and the signal from the recovering magnetization is acquired at a specified later time (defined as the inversion time TI). Images are acquired at several TI values in order to generate a magnetization recovery curve at each pixel. Since the arterial spins entering the slice are not influenced by these selective inversion pulses, they enter the slice with full longitudinal magnetization (i.e. they are in thermal equilibrium). Then,

$$M_a(t) = M_a^0$$

where $M_a^0$ = the value of $M_a(t)$ at thermal equilibrium. In the two-component model, we assume that the arterial blood spins entering the slice mix thoroughly with spins in the surrounding breast tissue before leaving the slice. Thus,

$$f\, M_a^0 = f\, \frac{M_0}{\lambda}$$

and Eq. (1.2) becomes

$$\frac{dM(t)}{dt} = M_0(\frac{1}{T_1} + \frac{f}{\lambda}) - M(t)(\frac{1}{T_1} + \frac{f}{\lambda}) \tag{1.3}$$

A MR system measures the apparent $T_1$, here represented as $T_{1s}$, as if the all spins are stationary (not flowing):

$$\frac{dM(t)}{dt} = \frac{M_0 - M(t)}{T_{1s}}$$

where,

$$\frac{1}{T_{1s}} = b_s = \frac{1}{T_1} + \frac{f}{\lambda} \tag{1.4}$$

and the subscript $s$ denotes that the parameter was measured using the selective RF pulse.

Images are also acquired in a so-called "Non-selective Tagging Condition". Here, spins are inverted everywhere in the sensitive volume of the body coil, but signals are acquired only from the slice being investigated, as in the Selective Tagging Condition. The arterial spins flowing into the slice thus experience they same inversion pulses as those within the slice, and the magnetization of entering arterial blood can be written

$$f\, M_a(t) = f\, \frac{M(t)}{\lambda}$$

Eq. (1.2) reduces to the simple expression

$$\frac{dM(t)}{dt} = \frac{M_0 - M(t)}{T_1}$$

where $T_1$ in this case represents the true $T_1$ of the tissue without the confounding influence of blood flow. This $T_1$ and corresponding rate $b_n$ is denoted

$$T_{1n} = T_1 \tag{1.5}$$

and

$$b_n = \frac{1}{T_{1n}} \tag{1.6}$$

where the subscript $n$ is used to distinguish these parameters from those found in Selective Tagging Condition. Based on the $b_s$ and $b_n$ values obtained from the two tagging conditions, we can determine the perfusion parameter $f/\lambda$:

$$\frac{f}{\lambda} = b_s - b_n \tag{1.7}$$

This $f/\lambda$ is the rate of magnetization replacement in a voxel. The importance of $f/\lambda$ is that, compared to normal breast tissue and benign breast lesions, a higher $f/\lambda$ is expected in malignant tumors, due to higher blood flow rates into the malignant tumor.

Contributions to pulse sequence design

The University of California Davis Medical Center operates a Signa Advantage 1.5 T GE MR system (Milwaukee, Wisconsin) (with 1.0 g/cm peak gradient strength, 500 microsecond rise time, and version 5.4 OS) for MR clinical and basic science research. An arterial spin tagging pulse sequence has been developed for this MR system based on the original source code of the commercial GE 2D fast Spoiled Gradient Recalled Echo (SPGR) pulse sequence. In this sequence, after the inversion RF pulse, raw data is acquired for an entire 2D image using the fast SPGR k-space acquisition (**Figure 3**). Several innovations have been implemented in this custom pulse sequence: **1.** The original 2D fast SPGR data acquisition scheme has been modified to support a symmetric centric *k* space data acquisition. Data acquisition starts at the zero *ky* line of the *k* space, and alternates below and above this *ky* line, end at the highest frequency *ky* lines. This allows the low spatial frequency components, which have the dominant effect on image contrast, to be acquired at the beginning. The effective time of inversion, defined by the time from spin inversion to the acquisition of the center *k* space line, can be adjusted most flexibly with this acquisition. **2.** Implementation of an optimized RF inversion pulse and an optimized RF acquisition pulse, both derived from the Shinnar Le-Roux (SLR) algorithm [28]. These optimized RF pulses allow slice profiles with sharp edges so that, in the selective condition, the alignment between the inversion slice and the image slice is as good a match as physically possible. Sections of inverted magnetization (slabs) are created by applying SLR inversion pulses in the presence of slice selection gradients. The inversion slab thickness is controlled by

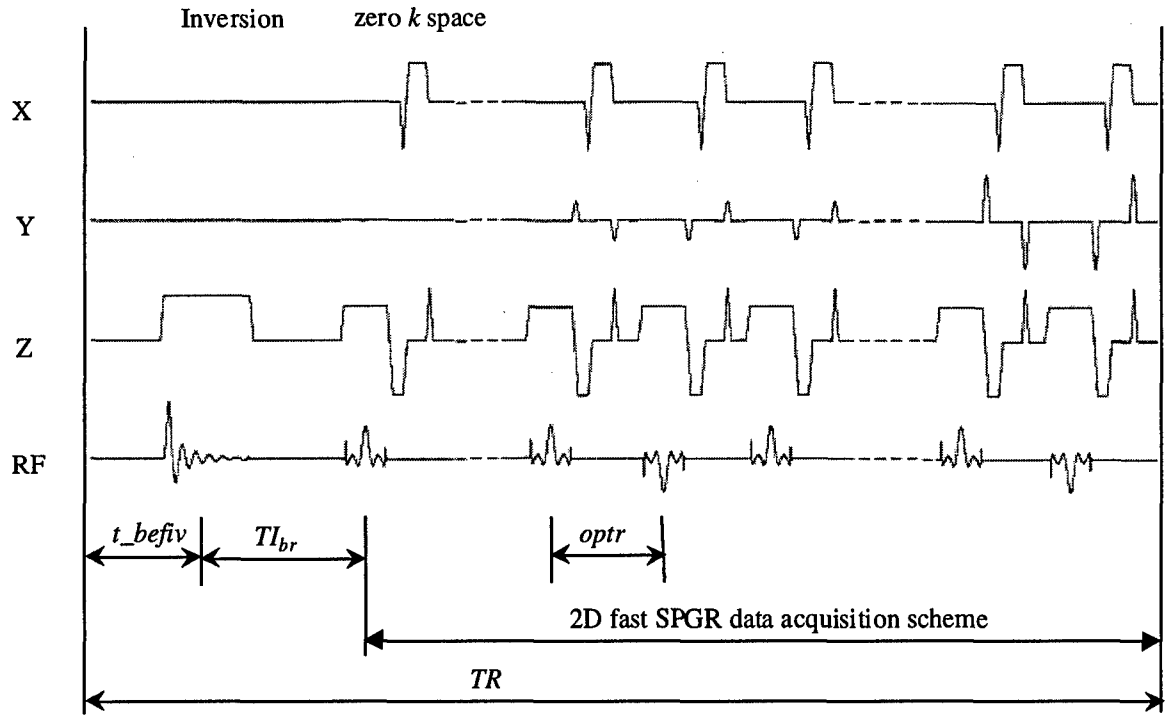


Figure 3. Spin-tagging sequence. *TR* is fixed at 2.7 sec. In each TR interval, an inversion RF pulse is applied first, followed by phase encoding steps starting at zero *k* space. The time $TI_{br}$ is changed by changing the pulse sequence control variable *t_befiv*. The RF pulses are magnified, and *t_befiv* and $TI_{br}$ are not to scale (actually longer than shown).

changing the gradient strength. By applying the SLR pulse without an associated slice selection gradient, a non-selective slab containing inverted spins in the entire sensitive volume of the transmit RF coil is created. By applying the pulse with the gradient, a selective slab of specific thickness is created. **3.** The so-called odd-number interleaved *k*-space acquisition [29,30] has been implemented to allow high spatial resolution in the phase encoding direction. With this acquisition, temporal resolution can be traded for image spatial resolution. Overall, the time required to acquire an arterial spin tagging image at a single slice is 2 minutes 30 seconds. This longer time than originally proposed is due to the fact that images at a multitude of TI times were needed to accurately estimate the contribution of blood flow the apparent longitudinal relaxation time, and thus to estimate perfusion.

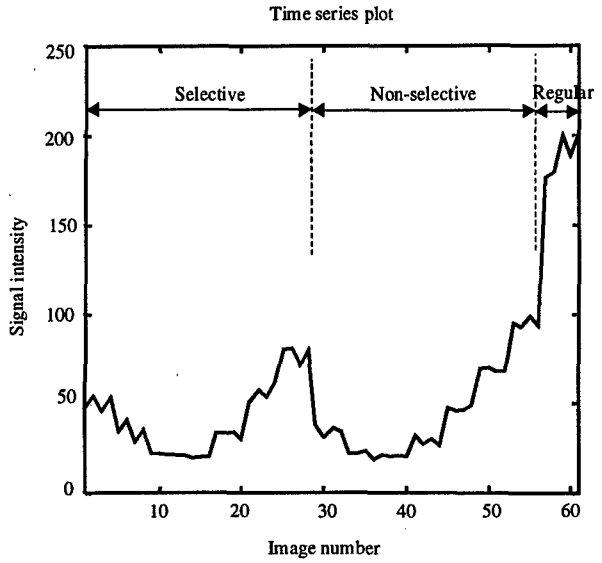


Figure.4. Signal intensity timeseries of one pixel across 61 images acquired using the spin tagging sequence. Selective, Non-selective and Regular Tagging Conditions are shown. For Selective and Non-selective Conditions, images are acquired with seven different *TI* s in each, and four images are acquired at each *TI* . Images are acquired in a without pausing with TR = 2.7 seconds.

Our protocol using the pulse sequences

The protocol has been modified from that described in the proposal, to account for the longer scan time required for the spin tagging sequence. For each subject, 10 or more equally spaced slices in the breasts are analyzed. Breasts are scanned bilaterally. A dual phased array breast imaging RF coil (Medical Advance, Inc., consigned specifically for this project) is used for the breast studies. Spin tagging measurement is based on three conditions during image acquisition: 1. selective inversion slab on (Selective Condition), 2. non-inversion slab on (Non-selective Condition), and 3. no inversion slab (Regular Condition). At each slice, a time series of 61 images are acquired with a fixed time of repetition (*TR*) of 2.7 seconds, with a total scan time of about 3 minutes. At each time series, Conditions 1, 2 and 3 are applied in sequence. For either the Selective or Non-selective condition, there are seven *TI* cycles with seven different *TI*'s (interval between the spin inversion and the effective center of *k* space of each image acquisition). In each *TI* cycle, four images are acquired. For the Regular Condition, five images are acquired (**Figure 4**). Repeated image acquisition with the identical parameters is done to improve the signal-to-noise ratio (SNR). The total scan time for the whole scan of 12 slice locations is about 30 minutes.

Contributions to data analysis

A data analysis technique described below has been developed from scratch (no prior description in the literature) to properly interpret the timeseries of signal changes obtained at each pixel. It has been developed taking into account the characteristics of 2D fast SPGR data acquisition. The analysis rests on the assumption that the 2D fast SPGR data acquisition does not disturb the recovery curve of the inverted spins or the equilibrium states of non-inverted spins. Although not strictly true, the deviation from reality does not significantly affect the outcome of the

measurements. Using images obtained under the "Regular" and the Selective or Non-selective Tagging Conditions, $T_{1s}$ or $T_{1n}$ is calculated at each pixel using a semi-log linear regression (**Figure 5**),

$$\frac{1}{T_{1s}} = -\frac{\ln(S_{reg} - S_{sel}(i)) - \ln(S_{reg} - S_{sel}(j))}{TI_{br}(i) - TI_{br}(j)} \quad (1.8)$$

and

$$\frac{1}{T_{1n}} = -\frac{\ln(S_{reg} - S_{non}(i)) - \ln(S_{reg} - S_{non}(j))}{TI_{br}(i) - TI_{br}(j)} \quad (1.9)$$

where $S_{reg}$ = the average steady-state signal intensity at a pixel under the Regular Condition, $TI_{br}(i)$ = the ith effective inversion time (TI) (used for the ith image), $S_{sel}(i)$ = the steady-state signal intensity at a pixel under the Selective Condition using the ith TI, and $S_{non}(i)$ = the steady-state signal intensity at a pixel under the Non-selective Condition using the ith TI. According to the theory (reviewed above), the value of $f/\lambda$ is the difference between the inverse of the $T_1$ values as expressed in Eq.(1.7). A derivation of the above linear regression equations is given in the Appendix.

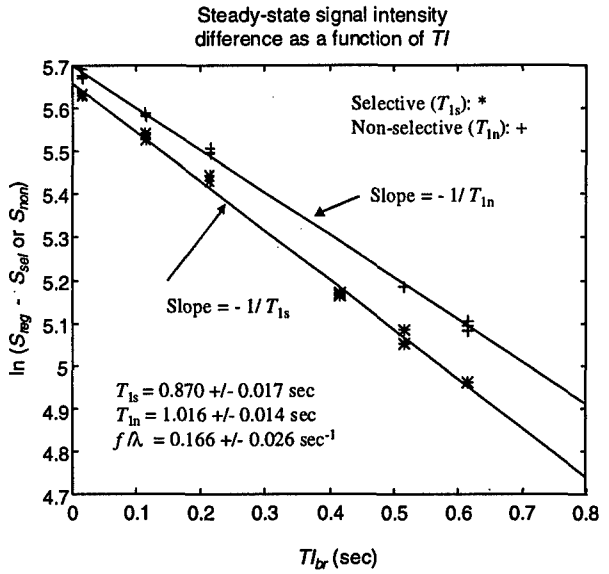


$TI_{br}$ = Start of image acquisition, measured from time magnetization is inverted; $S_{reg}$ = Average signal from last three images during Regular Tagging Condition; $S_{sel}$ = Signal from steady-state image during Selective Tagging Condition; $S_{non}$ = Signal from steady-state image during Non-selective Tagging Condition.

Figure 5. Example semi-log linear regression method for calculating $T_1$ values ($T_{1s}$ for Selective Tagging Condition, and $T_{1n}$ for Non-selective Condition) and effective perfusion $f/\lambda$. The calculation is based on the number of points remaining after use of minimum-mean-square-error technique to remove outliers.

As mentioned previously, four images are acquired for each *TI* under the Selective Condition, four images are required for each *TI* under the Non-selective Condition, and five images are acquired under the Regular Condition. Generally, we have observed that only the last three repeated images are at the steady state for their particular condition. The first two images the signal intensity is approaching the steady state. Therefore, only these last three are used for the above linear regression. A total of 21 data points are available for the calculation of $T_{1s}$ or $T_{1n}$, however, the three low signal data points near the zero-crossing line are unreliable and are usually eliminated (based on an outlier analysis). Finally, there are 18 remaining points for the calculation of the $T_1$s. Because the $T_1$ and $f/\lambda$ calculations based on this pulse sequence are very sensitive to structured and random noise, in particular the structured noise due to motion (pixel displacements), two noise-reduction techniques have been implemented. In the first technique, the resolution of each image is reduced from 256 x 256 to a lower resolution, for example, 64 x 64, by pixel averaging. This improves the signal-to-noise per pixel, and reduces the effect of small tissue motions occurring during the 61 images being analyzed. This reduction is due to the simple fact that any particular

motion results in a lower fractional change in the pixel volume. The second technique uses a data elimination strategy to reduce the mean-square-error of the semi-log regression used for determination of the $T_1$s. This technique permits the elimination of up to five noisy data points (out of 18) to reduce the $T_1$ regression error.

Contributions to image processing

A computer program, called BrView, has been developed for display, analysis, and interpretation of the images obtained in the breast imaging protocol, starting from previous programs developed by the PI for neuro-functional MRI research (as described in the proposal). The program is written in C, the X Window System, and Motif. For all of the analysis methods described above, the values of $T_{1s}$, $T_{1n}$ and $f/\lambda$ at different pixel locations on each slice are calculated. Images, which we call feature images, are formed based on these values. The three most useful feature images are those showing $T_{1n}$ values, the perfusion image showing $f/\lambda$ values, and the $f/\lambda$ error image based on the standard deviations of $f/\lambda$ values. These feature images contain pixels with a wide range of values. However, values of $T_1$, $f/\lambda$ and $f/\lambda$ errors of normal breast tissues are within narrow ranges, while pixels displacing large $f/\lambda$, $T_1$ above 500 ms, but small $f/\lambda$ error are regarded as suspicious of malignant disease. Pixels containing fat display very short $T_1$ and the perfusion values at these pixels tend to be inconsistent. To display these feature images, an appropriate positive shift, scaling and window size is applied [31].

This BrView program is used to display and interpret the feature images for identification of suspicious regions. Since a sizable breast lesion covers several pixels within the same slice and possibly neighboring slices, these pixels should have similar tissue characteristics. It is assumed that pixels with a breast lesion will have approximately equal $T_1$ values, and that these $T_1$ values will be relatively high compared to fat, and also show high perfusion rates with low perfusion standard errors. When a pixel is found to have a moderately long $T_1$, and a high $f/\lambda$, and the $f/\lambda$ error is low, surrounding pixels within the same slice and across slices are also checked to see if they have similar characteristics. The "suspicion index" for this pixel is defined as the percentage of surrounding pixels also classified as suspicious. By applying this method to all pixels in all slices, "suspicion index maps" are created. If the pixel has a suspicion index exceeding a threshold, this pixel would be highlighted on the display. Clearly, the level of suspicion here is qualitative. Neither a rigorous statistical analysis of the procedure, nor a statistical comparison and analysis of suspicion regions with the results of dynamic contrast enhanced MRI, has not been carried out yet. Nevertheless, the goal is to develop a quantitative tool for breast cancer detection. The suspicion index threshold for identification of malignant disease, as well as independent thresholds for $f/\lambda$, $T_1$ and the standard deviation of $f/\lambda$, should ultimately be based on the results of a large set of patient studies.

Based on the small set of studies that have been done, the thresholds used to identify suspicious pixels are as following:

$T_1$: $> 0.5$ sec
$f/\lambda$: $> 0.1$ sec$^{-1}$
STD of $f/\lambda$: $< 0.1$ sec$^{-1}$.

and the suspicion index threshold, used for asserting a "high" probability that the tissue is abnormal, is set at 20 %. A quantitative analysis of the false positive and negative error rates

associated with this threshold has not been done. The BrView program allows clinician researchers to change the thresholds and observe the changes in the suspicion index maps. This visualization program can simultaneously display feature images and standard clinical MR images. Parameters $T_1$, $f/\lambda$, and the standard deviation of $f/\lambda$ at any pixel location of the breast objects can be found by a click of the mouse on that location. If a dynamic contrast enhancement study has been done, a click of the mouse reveals a plot of the change of signal intensity as a function of time at this location. The suspicious regions can also be mapped to high-resolution traditional clinical images (256 x 256), which are always acquired for comparison during each subject study. This mapping provides a radiologist the traditional view of the breast images with the suspicious regions identified. In summary, BrView is designed to allow pixel cross-registration and comparison between results from different MR imaging techniques. It provides an efficient working environment for clinicians making diagnostic decisions.

Other image processing contributions are methods to reduce tissue misregistration that cause inaccuracy in the $T_1$ estimation. Breast images are expected to precisely align in all 61 images

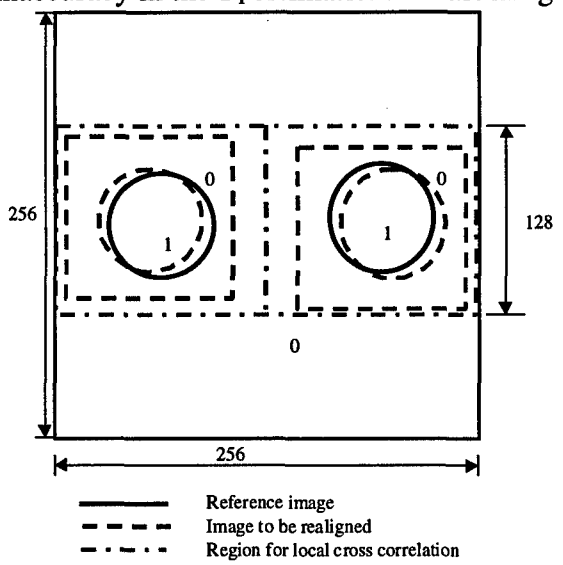


Figure 6. Local cross correlation is performed between the binary image and reference binary image. The maximum correlation occurs when the two objects maximally overlap.

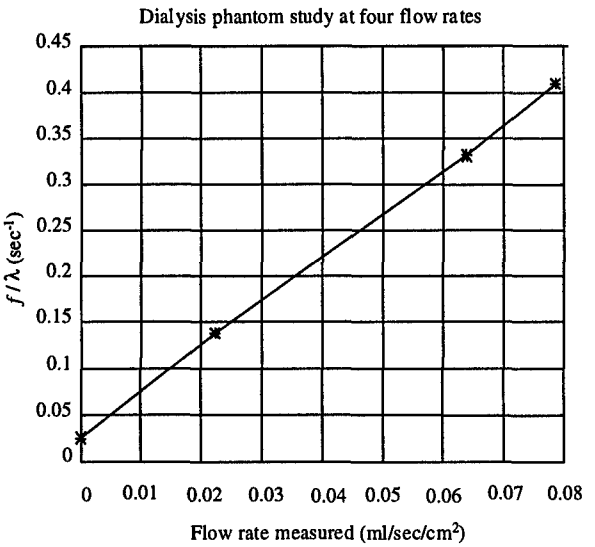


Figure 7. Kidney dialysis phantom flow study: Arterial spin-tagging was applied at four different flow rates: 0, 0.0222, 0.0640 and 0.0787 ml/sec/cm$^2$. The corresponding calculated $f/\lambda$ values were 0.0251, 0.138, 0.331 and 0.409 sec$^{-1}$.

acquired in the timeseries at each slice location. Unfortunately, the patient may move during the two minute 30 second scan, resulting in a change in breast position and orientation. The motion estimation used here is based on binary segmentation, following by statistical best-fit alignment of defined regions across the collection of 61 images. Geometric constraints of patient motion and breasts, within the scanner and dedicated RF coil, suggest that only lateral displacements in the X and Y directions should be considered. The studies performed suggest that typical displacements are not large, within 1 cm. Such motions are correctable with segmentation and region alignment (see **Figure 6**).

Results of in-vitro and in-vivo testing

The success of the arterial spin tagging pulse sequence in measuring perfusion was first proven by the result of flow phantom studies. All studies showed that there was a linear relationship

between $f/\lambda$ and actual flow. All evaluated flows were within the range of tissue perfusion (**Figure 7**). Furthermore, the $T_{1n}$ values obtained in the non-selective condition, at four different flow rates, were as expected, specifically 1.232 +/- 0.034 sec. A brain imaging study was performed to further evaluate the arterial spin tagging pulse sequence. In 11 different regions of interest (ROIs), defined at several different slice locations, white matter had $T_{1n}$ equal to 0.495 +/- 0.021 sec, $T_{1s}$ equal to 0.487 +/- 0.022 sec, and $f/\lambda$ equal to 0.030 +/- 0.075 sec $^{-1}$, ranging from 0 to 0.131 sec $^{-1}$. Gray matter in this study had $T_{1n}$ equal to 0.665 +/- 0.065 sec, $T_{1s}$ equal to 0.629 +/- 0.035 sec, and $f/\lambda$ equal to 0.081 +/- 0.054 sec $^{-1}$, ranging from 0.037 to 0.170 sec $^{-1}$. In two normal breast studies, at 14 different ROIs defined at several different locations, parenchyma (glandular tissue) had $T_{1n}$ equal to 0.772 +/- 0.088 sec, $T_{1s}$ equal to 0.709 +/- 0.062 sec, and $f/\lambda$ equal to 0.109 +/- 0.053 sec $^{-1}$, ranging from 0.043 to 0.190 sec$^{-1}$. Normal fat tissue had $T_{1n}$ equal to 0.377 +/- 0.069 sec, $T_{1s}$ equal to 0.363 +/- 0.056 sec, and $f/\lambda$ equal to 0.086 +/- 0.073 sec $^{-1}$, ranging from 0.003 to 0.177 sec $^{-1}$. The values resulting from the head and normal breast studies were within expected ranges.

Results of patient studies

### Introduction

For this and all cases summarized below, suspicious pixels were identified based on the following criteria:

$T_1$: > 0.5 sec
$f/\lambda$: > 0.1 sec$^{-1}$
STD of $f/\lambda$: < 0.1 sec$^{-1}$.

and the suspicion index threshold was set at 20.2 %. Analysis was done using the program BrView.

### Case 1

Case Study #1: palpable mass
Date of study: Dec 10, 1997
Level of suspicion based on $T_{1n}$ and perfusion: Moderately High
Clinical MR images: Negative (lesion not visualized)
Assessment based on spin tagging: Positive for malignancy
Biopsy result: benign (spin tagging INCONSISTENT with biopsy)

Discussion: **Figure 8** shows the three feature images, and an image acquired under the "Regular Tagging Condition" of the arterial spin tagging sequence. All three feature images are 64 x 64. The $T_1$ image has excellent SNR and clearly shows the distribution of $T_1$ values. In particular, bright areas at the centers of the breasts represent glandular tissue with long $T_1$ values. The corresponding perfusion image has relatively low SNR. Some pixels at the edge of the breasts have high intensity due to high calculation error, not high $f/\lambda$. The calculation at edge pixels is extremely sensitive to breast motion, as well as to the presence of Gibbs ringing artifacts common in low resolution images. Pixels with high $T_1$ values generally have less perfusion error. Because the perfusion estimates are more sensitive to errors in $T_1$ when $T_1$ is low. Fortunately, this property of the error should not limit the identification of malignant tissue very much, because malignant tissue will typically have relatively high $T_1$ values (> 500 ms). **Figure 9** shows the overlay of the suspicious regions onto the high-resolution clinical images. Highlighted

(pure white) pixels on the left breast (right side of image) on slices 4, 5, 6 and 7 may be identifying one contiguous mass. Physical examination of this patient revealed a mass at the nine o'clock position in the left breast, consistent with the suspicious cancer region identified by spin tagging.

### Case 2

Case Study #2: palpable mass
Date of study: Nov 16, 1997
Level of suspicion based on $T_{1n}$ and perfusion: Low
Clinical MR images: Positive (lesion visualized, consistent with palpation)
Assessment based on spin tagging: Negative for malignancy
Biopsy result: benign (spin tagging CONSISTENT with biopsy)

Discussion: The low suspicion index, based on $T_1$ relaxation time and perfusion, at and around the palpated lesion location was strong indication that the lesion was benign. Only one suspicious pixel was found at that location at the 20.2% threshold. It was judged that the breasts did not contain malignant tissue. This case is shown in **Figures 10(a)-(d)**.

### Case 3

Case Study #3: Palpable mass
Date of study: Aug 6, 1997
Level of suspicion based on $T_{1n}$ and perfusion: High
Clinical MR images: Negative (mass not clearly visualized, prior cyst visualized)
Result based on spin tagging: Positive for malignancy
Biopsy result: Positive (spin tagging CONSISTENT with biopsy)

Discussion: The high suspicion index, based on $T_1$ relaxation time and perfusion, at and around the lesion detected by palpation, was strong indication that the lesion was malignant. This case is shown in **Figures 11(a)-(d)**.

### Case 4

Case Study #4: Palpable mass
Date of study: Aug 7, 1998
Level of suspicion based on $T_{1n}$ and perfusion: High
Clinical MR images: Positive (lesion visualized)
Assessment based on spin tagging: Positive for malignancy
Assessment based on dynamic contrast-enhanced study: Positive for malignancy
Biopsy result: Negative (spin tagging NOT CONSISTENT with biopsy)

Discussion: High suspicion indices, based on relaxation time and perfusion, were found in several breast regions. The visible lesion location on clinical MRI was consistent with that of the palpable mass. It overlapped but was considerably smaller than that found by the suspicion indices. First-pass contrast enhancement study results correlated strongly with the high perfusion regions detected by spin tagging. Nevertheless, biopsy showed the mass to be benign. This case is shown in **Figures 12(a)-(d)**.

In summary, there was only partial agreement (2 of 4) between spin tagging and biopsy assessments of malignant disease. More patient studies (as planned in project), as well as follow-up of patients, is needed. Spin tagging may be detecting abnormal regions not evaluated by the

biopsies. Arterial spin tagging results were, subjectively, more convincing if the suspicious regions overlapped abnormal regions seen on standard clinical $T_1$, $T_2$ and proton-density weighted images. Unfortunately, standard clinical images often did not reveal any abnormal tissue, concurring with the view that standard clinical MRI is not definitive in the assessment of breast lesions. Dynamic first-pass contrast-enhanced imaging is definitely needed to help validate the spin tagging technique, and this imaging will be done on all subsequent patients in this project. In addition, results from X-ray mammography and ultrasonography will be compared, as has been done for prior studies (see page 40).

### *Future Implementations*

Arterial spin tagging with an echo planar type data acquisition

To derive the semi-log regression analysis, it was assumed that SPGR data acquisition would not disrupt the recovery of longitudinal magnetization of inverted spins, nor the equilibrium of the non-inverted spins. Unfortunately, this assumption is a cause of error in the method, and our simulations have shown that the $T_1$ calculated based on the assumption was slightly lower than the true $T_1$. Using the simulation results, a conversion table was developed to convert the estimate derived based on the assumption to a better T1 estimate. Nevertheless, a better approach would be to replace the 2D fast SPGR data acquisition scheme with an echo planar data acquisition scheme. Echo planar imaging (EPI), requires only a single RF pulse for acquisition of the entire data set for one image. The disturbance due to the repeated RF pulses to the recovery curves of the inverted spins or the equilibrium states of the non-inverted spins would be much more predictable. Also, EPI is faster than 2D fast SPGR, so the *TI* cycles could be redesigned, and a multi-slice technique introduced, to shorten the scan time by a factor of 4-8. This implementation would make possible high resolution scanning of the entire breast tissue in under 10 minutes. Starting September 1998, the UC Davis Medical Center will operate a GE Signa Horizon Echospeed MR system. This system will be capable of echo planar imaging (128 x 128 single shot is typical, but up to 256 x 256 single shot can be done). Conversion of the arterial spin tagging sequence to incorporate echo planar acquisition will be carried out. In addition, conversion will also be done for the existing spin tagging sequence that is based on 2D fast SPGR.

Magnetization transfer implementation

The second major assumption, used in the derivation of the perfusion formula, is that the contribution of the magnetization transfer term in Eq. (1.1) is negligible. To allow inclusion of this term, the spin tagging pulse sequence must include a binomial or high order RF pulse to prepare the spins prior to data acquisition. Differential magnetization transfer effects have been detected in head and neck neoplasms [32]. Development of this pulse sequence modification to estimate the size of the magnetization transfer contribution will be completed.

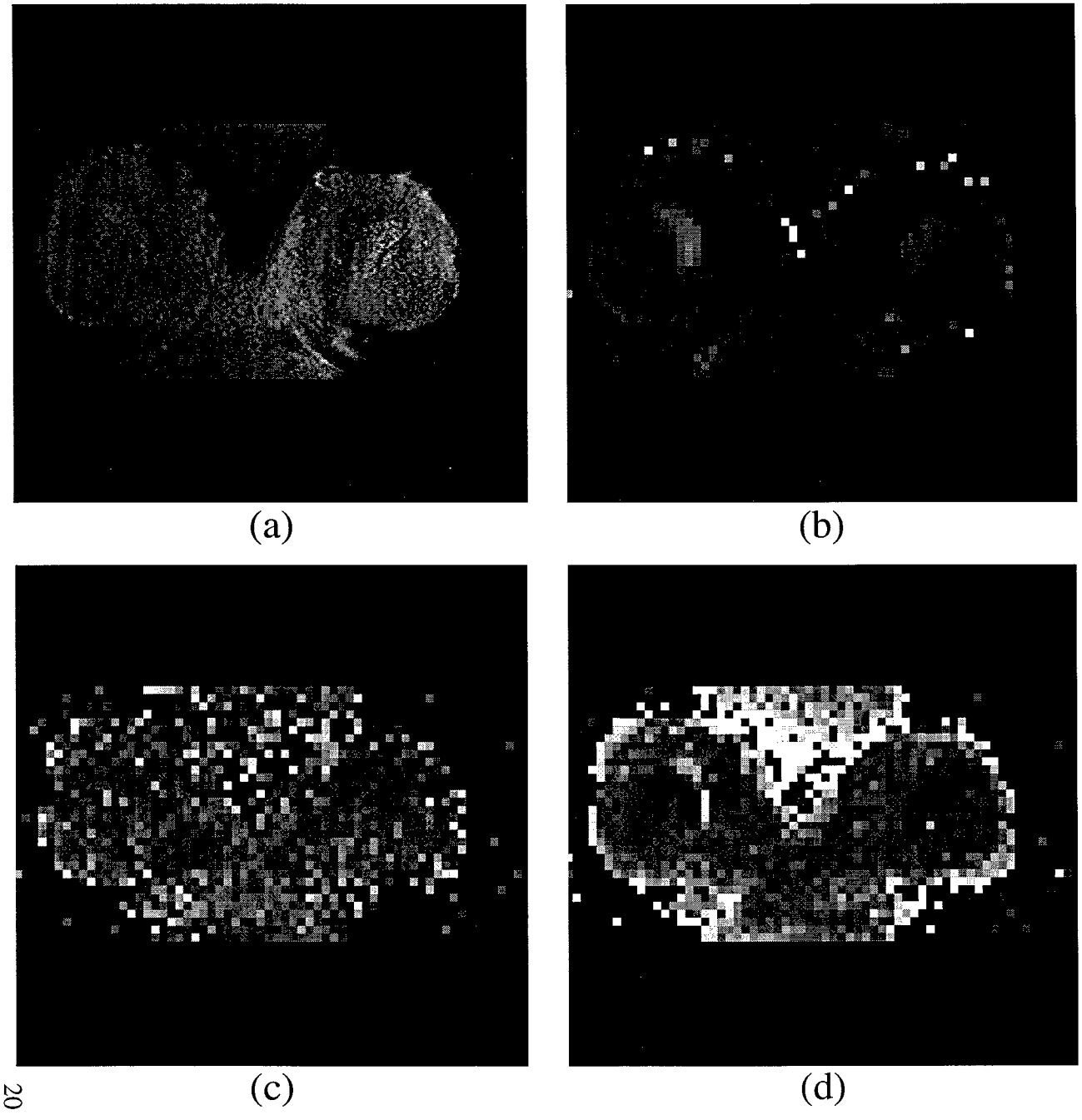


**Figure 8.** Dec 10, 1997. Example of feature images derived at single slice. (a) Image obtained during spin tagging sequence during Regular Tagging Condition. (b) $T_1$ image derived, at each pixel, from best-fit of signal intensity from sequence of images obtained at different inversion times (*TI*). (c) Perfusion ($f/\lambda$) image derived from comparison of $T_1$ images during Non-selective and Selective Tagging Conditions. (d) Perfusion error image, measured as standard error based on $T_1$ standard errors.

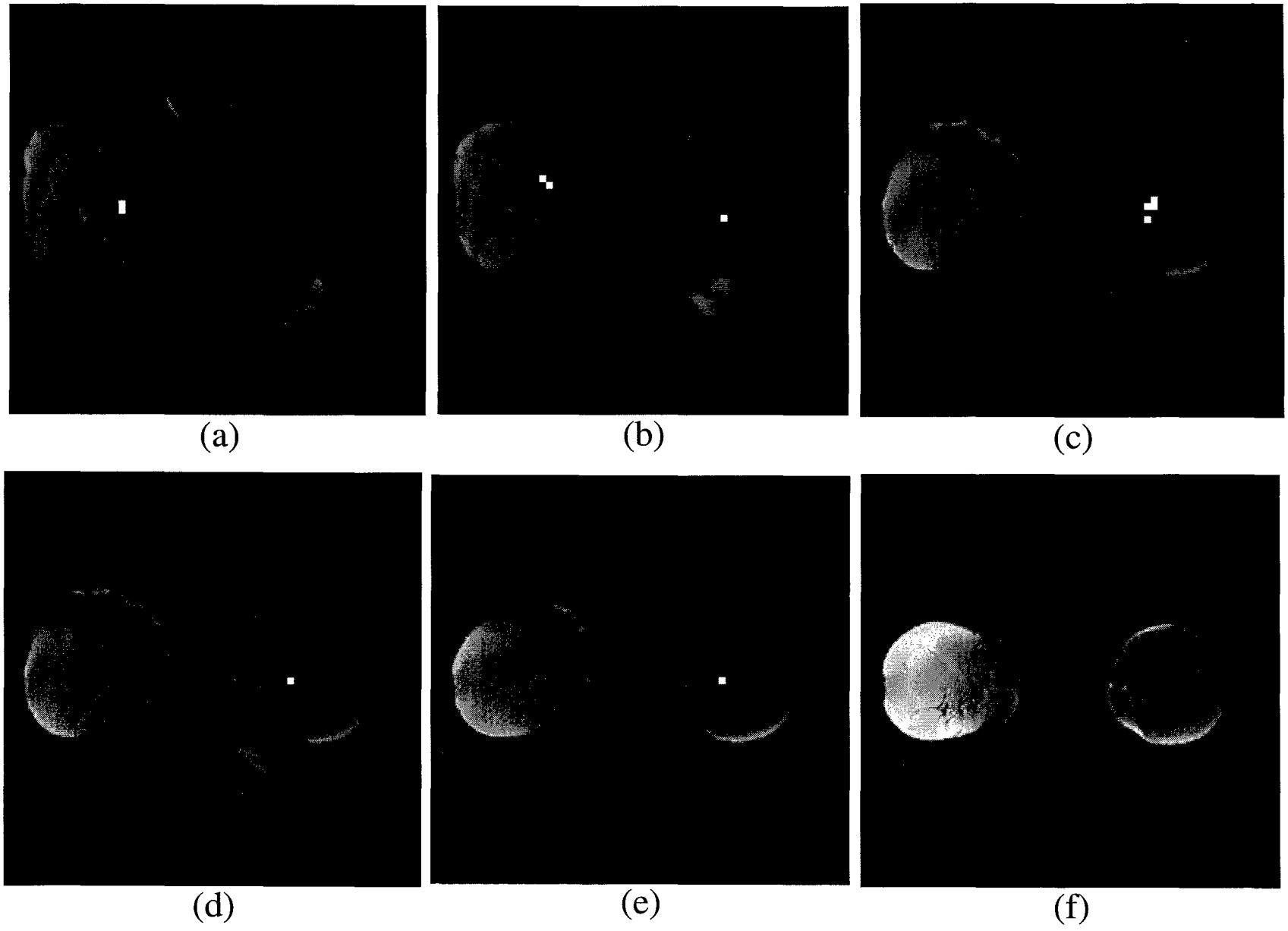


**Figure 9.** Dec 10, 1997 study. The suspicious pixels (threshold 20.2%), showing moderate $T_1$ , high $f/\lambda$, low $f/\lambda$ error, are identified on six (a-f) contiguous slices, displayed on fat suppressed $T_2$ weighted fast spin echo images.

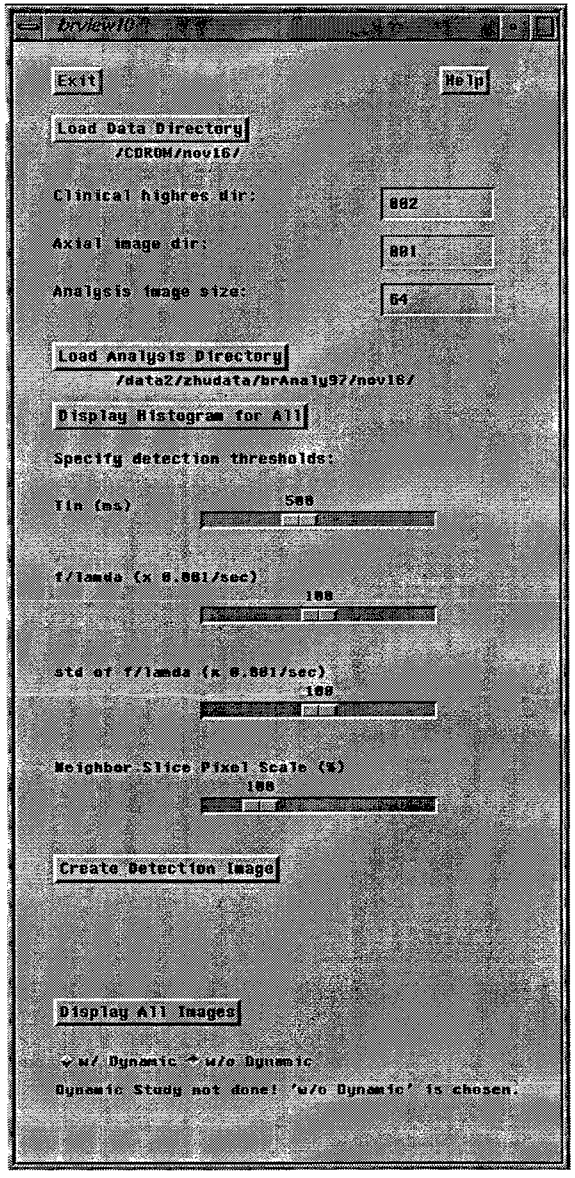


**Figure 10(a).** Nov 16, 1997 study. Suspicion index map is created using the "Create Detection Image" button after setting thresholds.

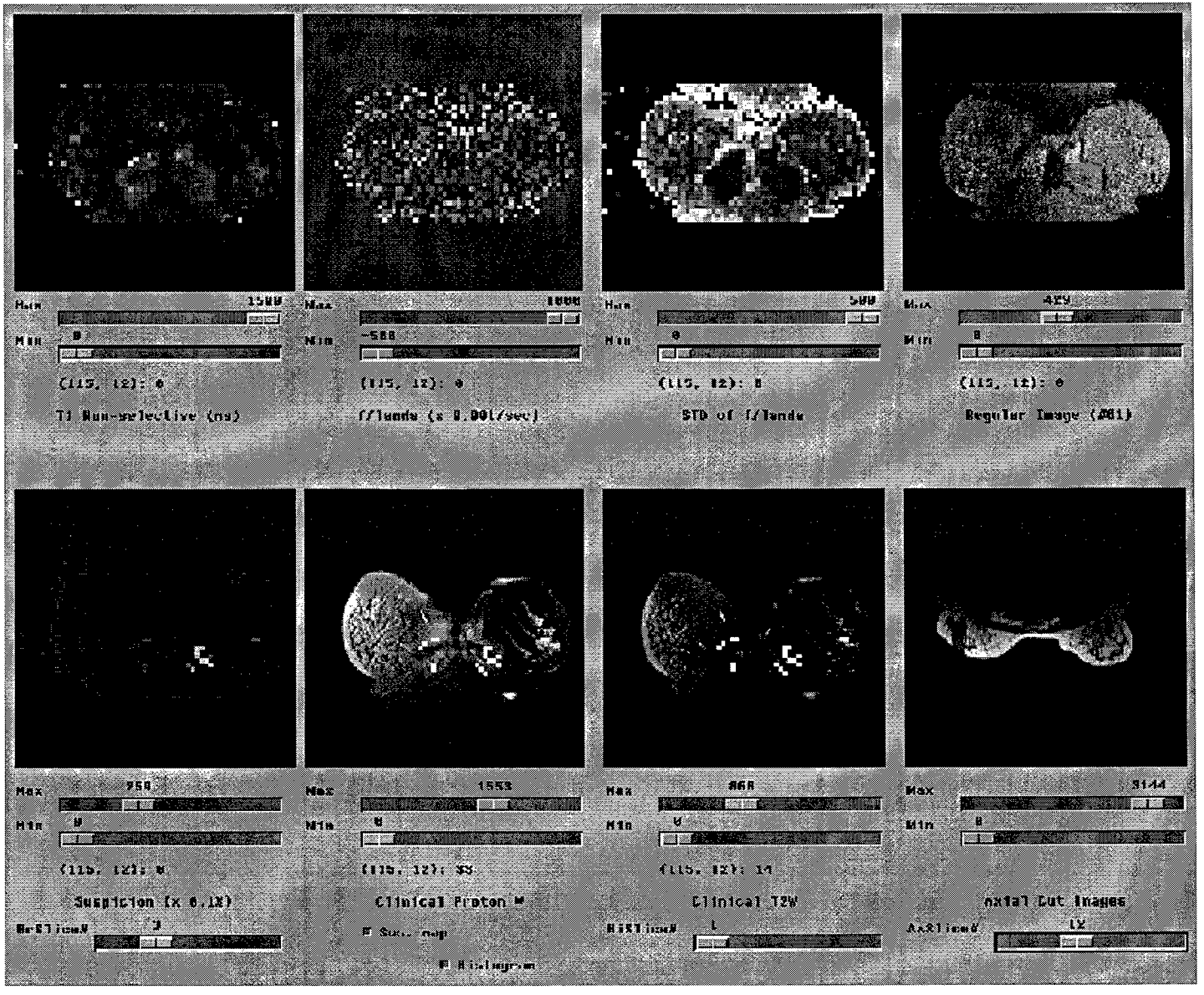


**Figure 10(b).** Nov 16, 1997 study. Feature images (top row), suspicion index map (bottom left, threshold 0.5%) and mapping (pure white pixels) of the map on proton density and $T_2$ images (bottom row). Also shown: Axial $T_1$.

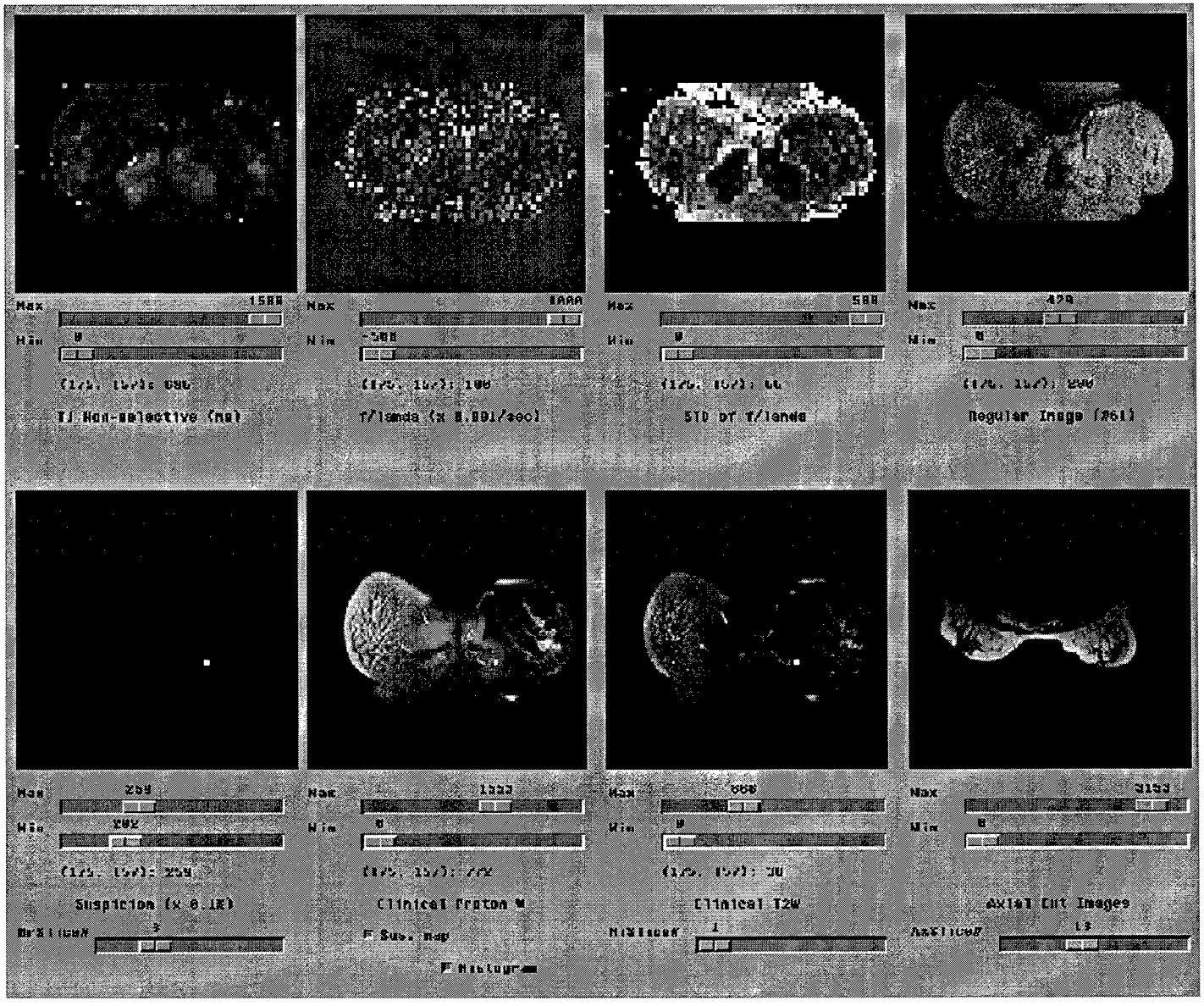


**Figure 10(c).** Nov. 16, 1997 study. Feature images (top row), suspicion map with the suspicion index threshold at 20.2% (revealing single pixel) and mapping (pure white pixel) onto proton density and $T_2$ images. Clicking on pixels displays numerical $T_1$, $f/\lambda$, standard error of $f/\lambda$, and suspicion index. Also shown: Axial $T_1$.

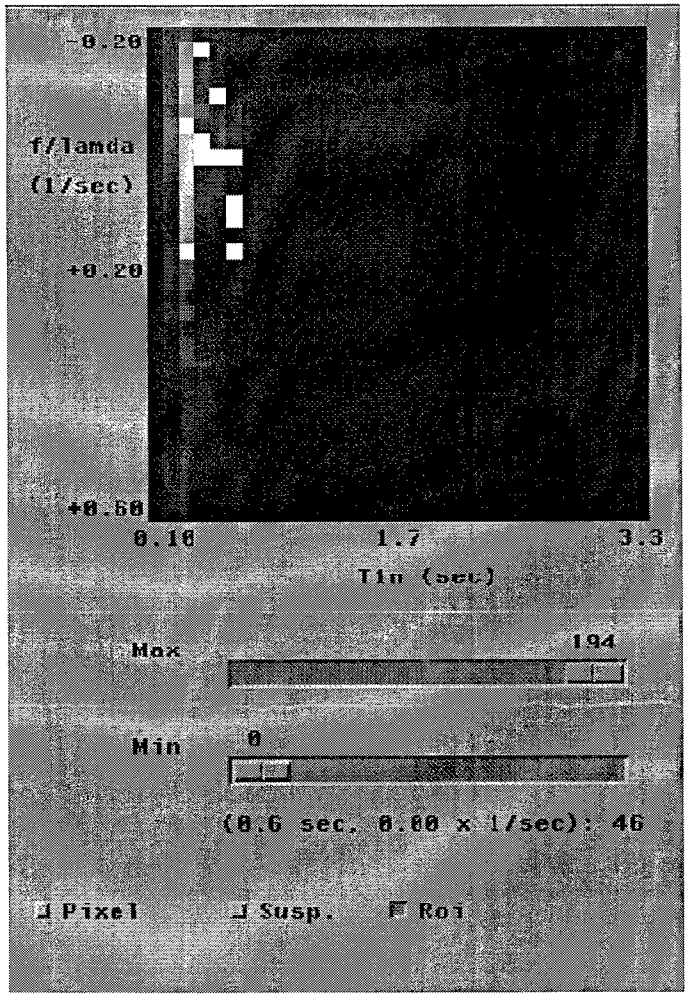


**Figure 10(d).** Nov. 16, 1997 study. The $T_1$ and $f/\lambda$ values of pixels representing the lesion identified by proton density and $T_2$ images, are superimposed on the histogram of the $T_1$ and $f/\lambda$ values from the entire breast. Shows that criteria for suspicuous pixels is based on moderate $T_1$ and high $f/\lambda$. See text for complete criteria.

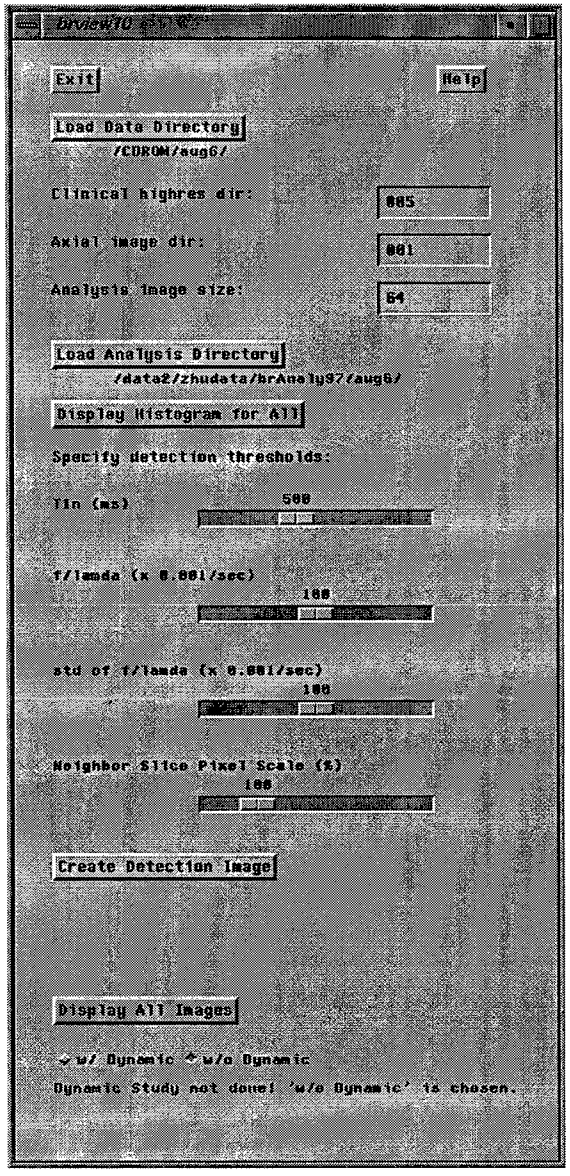


**Figure 11(a).** Aug 6, 1997 study. Suspicion index map is created using the "Create Detection Image" button after setting thresholds.

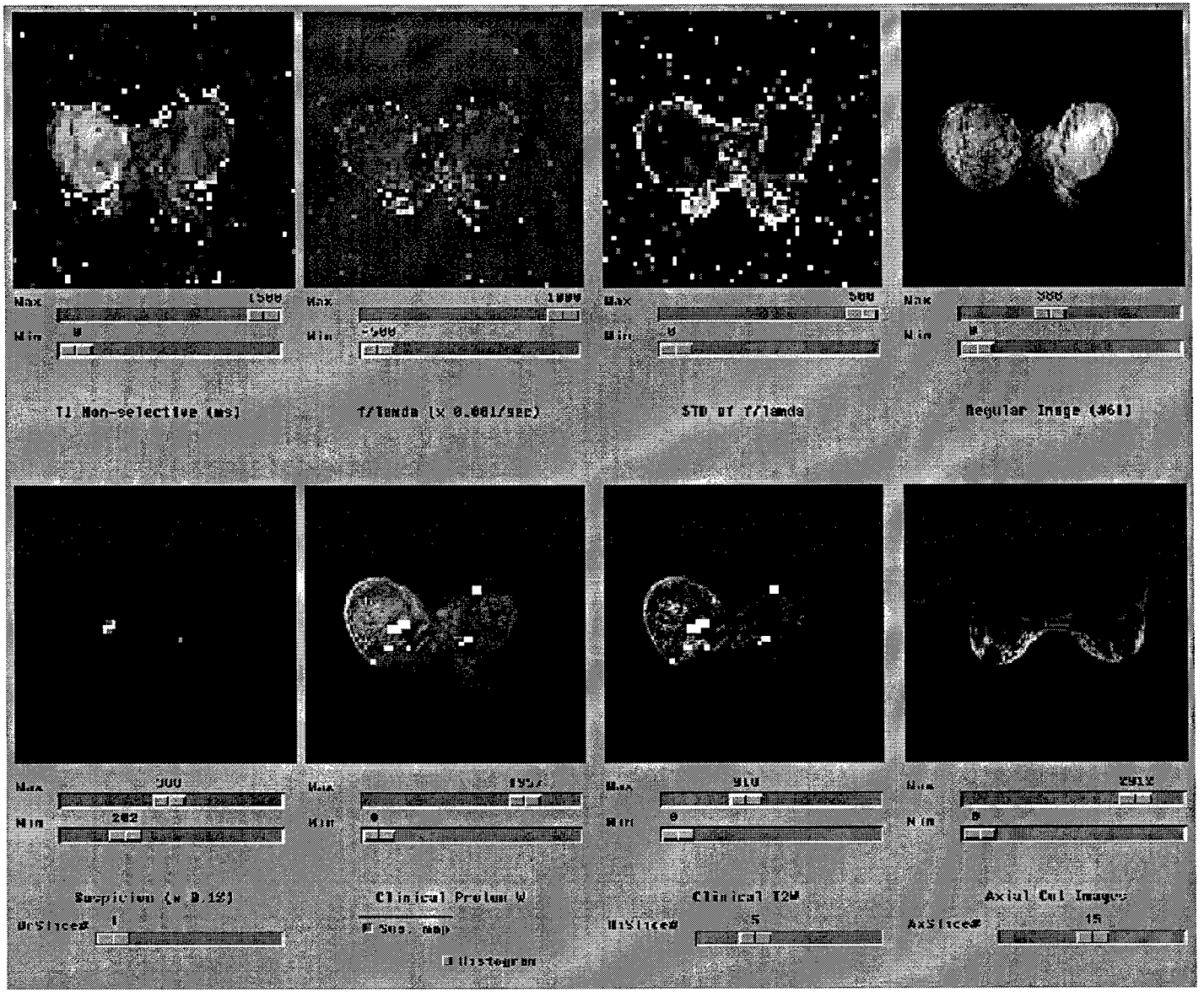


**Figure 11(b).** Aug 6, 1997 study. Feature images (top row), suspicion index map (bottom left, threshold 20.2%) and mapping (pure white pixels) on proton density and $T_2$ images. (bottom row). Also shown: Axial $T_1$.

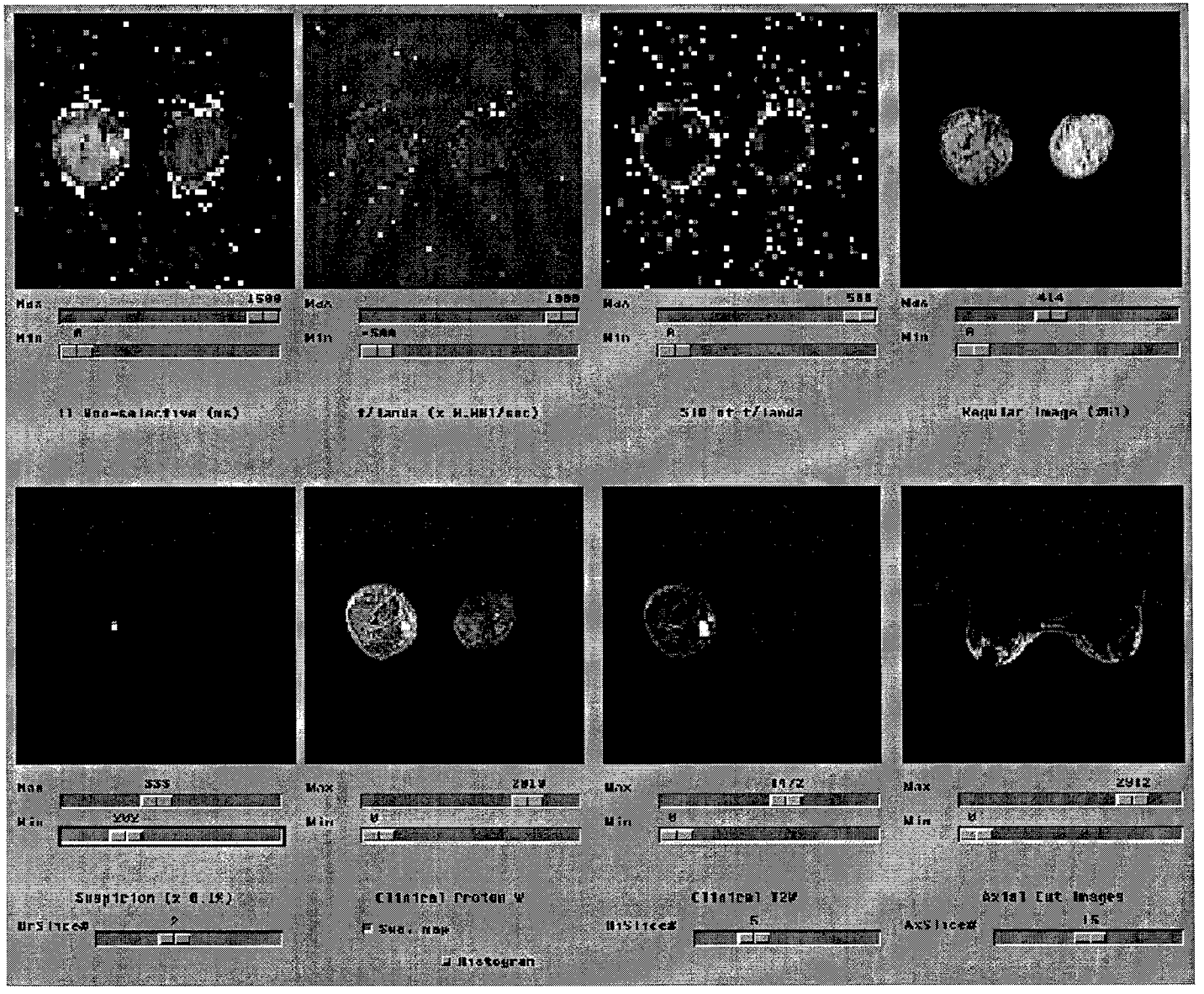


**Figure 11(c).** Aug 6, 1997 study, slice adjacent to that shown in Figure 11(b). Feature images (top row), suspicion index map with threshold at 20.2%, and mapping (pure white pixels) onto proton density and T2 images. Also shown: Axial $T_1$.

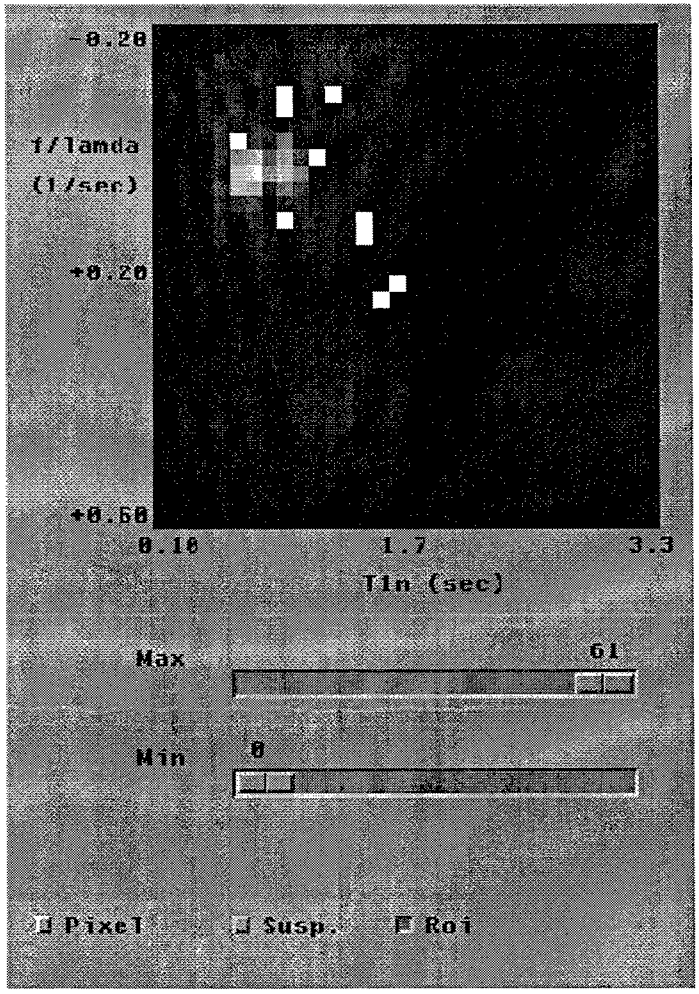


**Figure 11(d).** Aug 6, 1997 study. The $T_1$ and $f/\lambda$ values of pixels representing the lesion identified by proton density and T2 images in Figure 11(c), are superimposed on the histogram of the $T_1$ and $f/\lambda$ values from the entire breast. Shows that criteria for suspicion is based on moderate $T_1$ and high $f/\lambda$. See text for complete criteria.

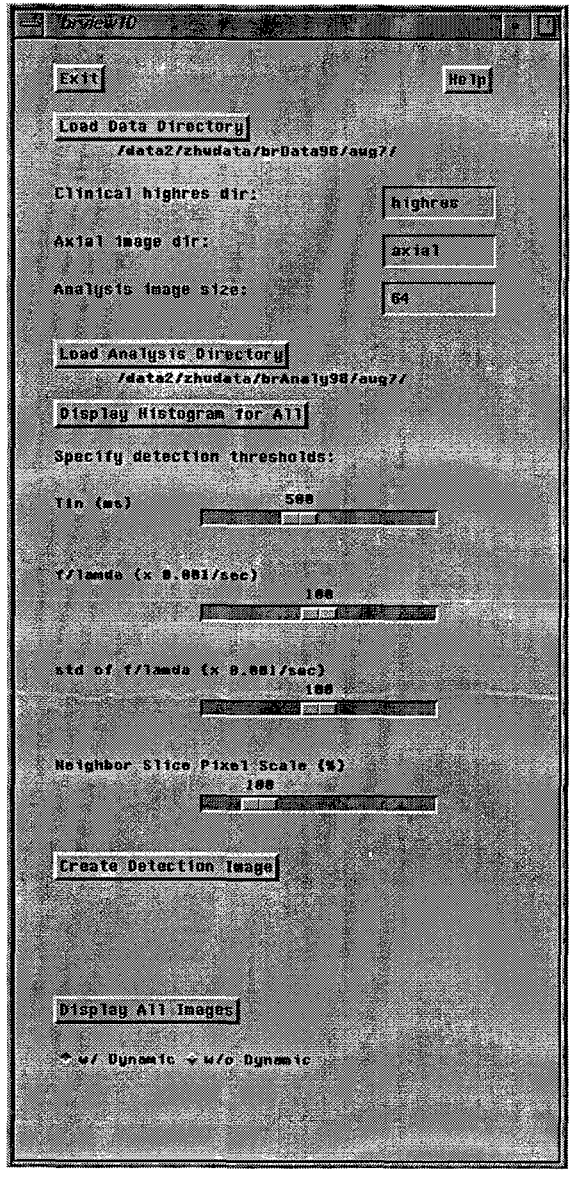


**Figure 12(a).** Aug 7, 1998 study. Suspicion index map is created using the "Create Detection Image" button after setting thresholds.

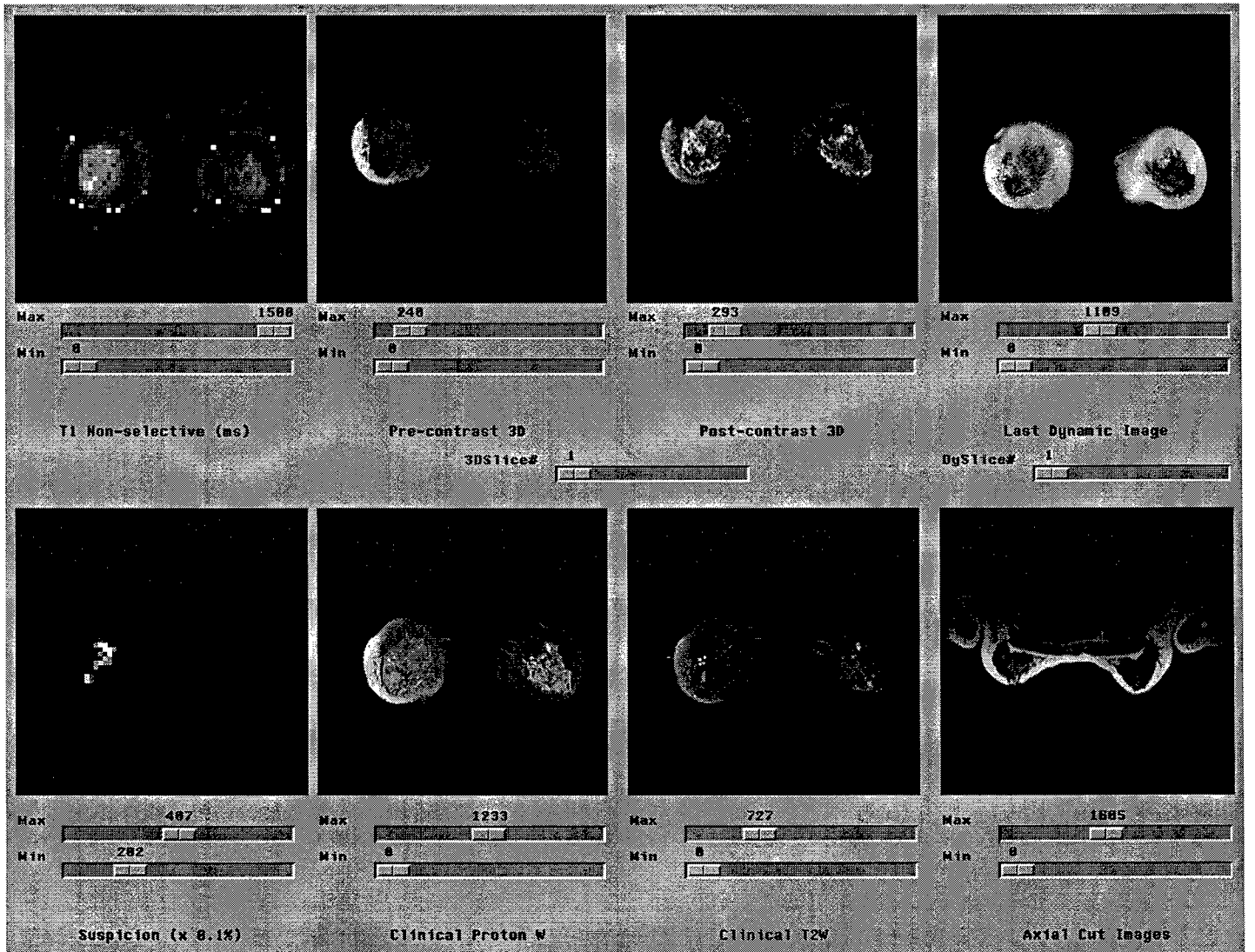


**Figure 12(b).** Aug 7, 1998 study. Feature images (top row), suspicion index map (bottom left, threshold 20.2%) Proton density, $T_2$, and $T_1$ images are shown without suspicion index map (bottom row). Also shown: Axial $T_1$.

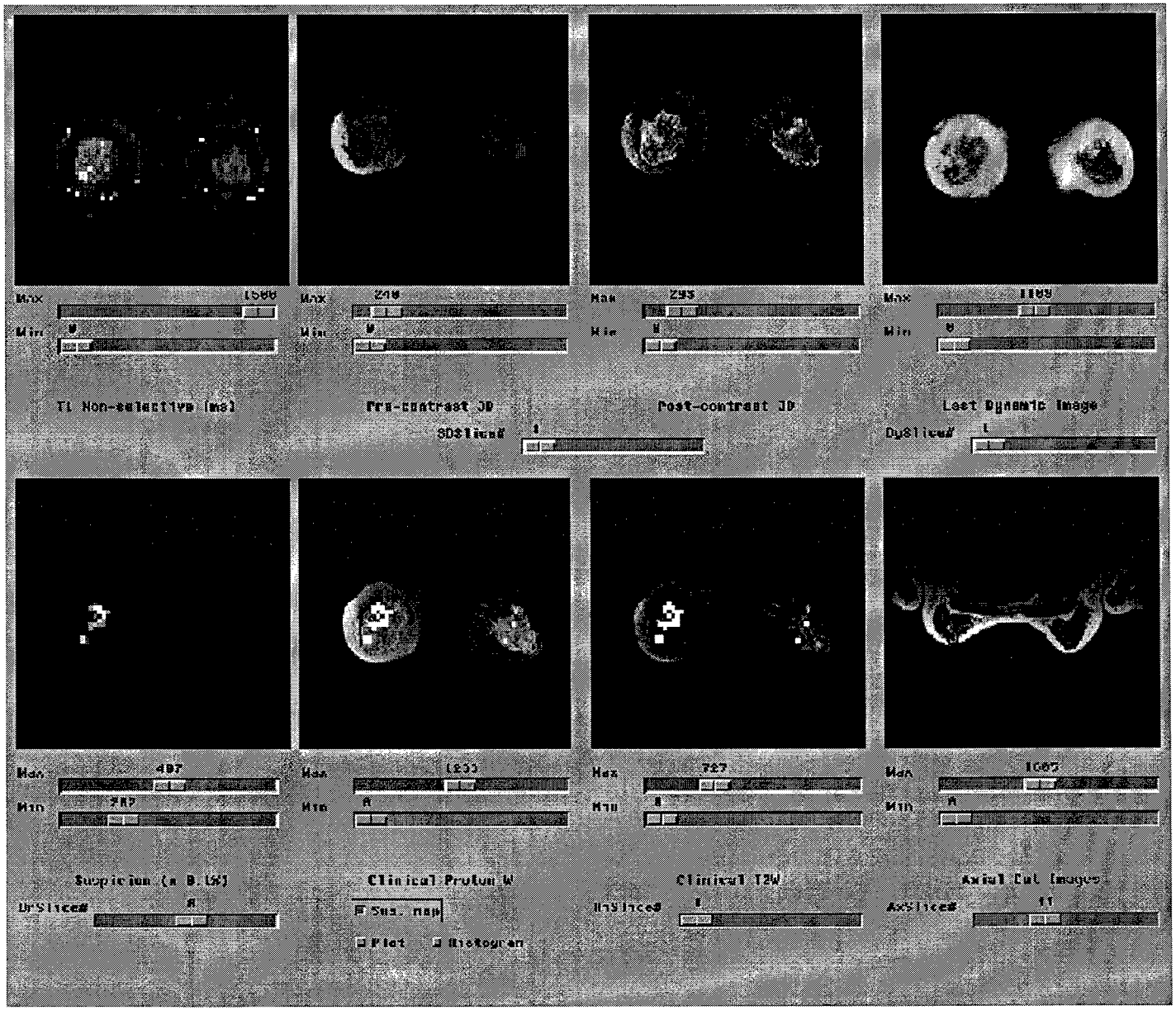


**Figure 12(c).** Aug 7, 1998 study. Feature images (top row), suspicion index map with threshold at 20.2% (revealing one cluster of pixels) and mapping (pure white pixels) onto proton density and $T_2$ images. Also shown: Axial $T_1$.

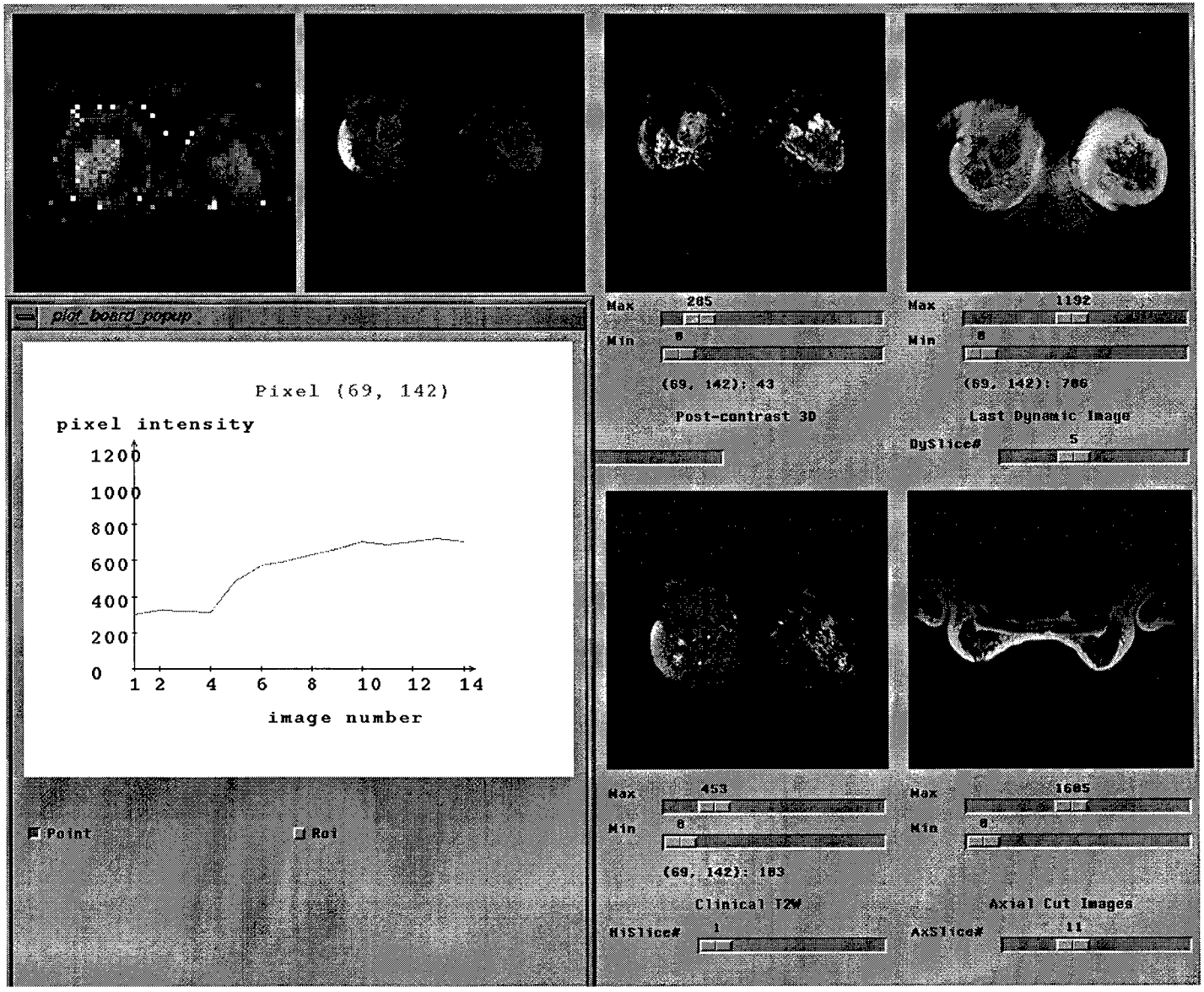


**Figure 12(d).** Aug 7, 1998. Timeseries of signal changes at a rapidly enhancing pixel during dynamic contrast enhancement. Also shown: $T_1$ "feature" image (1st from left), pre-contrast 3D image (2nd from left), and post-contrast 3D image, last image of dynamic study, $T_2$ image, and $T_1$ axial image.

## (7) CONCLUSIONS

In this year of the project, we have developed the necessary pulse sequences for anatomical and functional imaging of breast tissue, and the necessary software for the analysis, display and interpretation of this data. These developments will allow us to evaluate complete breast imaging studies that are composed of anatomical scans, dynamic first pass contrast enhanced scans, and arterial spin tagging scans. The integrated nature of the software allows easy and consistent interpretation of both spatial dependencies as well as temporal dependencies of signal changes indicative of disease. The in-vitro and in-vivo studies done thus far indicate that first and foremost, arterial spin tagging is a sensitive and reliable method for measuring $T_1$ and parameters related to tissue perfusion. Second, they indicate that arterial spin tagging is a viable alternative to dynamic first-pass contrast-enhanced imaging. The fact that arterial spin tagging can be easily added to any standard breast imaging protocol, without requiring special nursing or MR technologist expertise, means that it is especially attractive for routine clinical use. It could be used to supplement contrast-enhanced studies in the initial study of the patient, and used exclusively in follow-up studies. Since 10/1/98, six subjects have been studied without the dynamic first-pass contrast-enhanced scan, and two have been studied with this scan. Comparison of contrast-enhanced images versus arterial spin-tagged images has not yet been made. In particular, no statistical comparison of the dynamic study results (considered to be the gold standard for non-invasive assessment of malignant disease) and the arterial spin tagging results have been performed. However, there is considerable spatial overlap of suspicious regions obtained by these methods noted on visual inspection. Collecting data on human subjects, and statistical confirmation of this agreement, will be major focuses of next year's work.

## (8) REFERENCES


1. Heywang SH, Wolf A, Pruss E, et al: MR imaging of the breast with Gd-DTPA: use and limitations. Radiology 171: 95, 1989.

2. Kaiser WA, Zeitler E: MR imaging of the breast: Fast imaging sequences with and without Gd-DTPA: Preliminary observations. Radiology 170:681, 1989.

3. Fischer U, von Heyden D, Vosshenrich R, et al: Signal characteristics of malignant and benign lesions in dynamics 2D-MRI of the breast. Rofo Fortschritte auf dem Gebiete der Rontgenstrahlen und der Neuen Bildgebenden Verfahren, 1993, 158: 287.

4. Whitehouse GH, Moore NR. MR Imaging of the breast after surgery for breast cancer. In Magnetic Resonance Imaging Clinics of North America. Davis PE, Editor. WB Saunders. November 1994, 2 (4): 591-603.

5. Hickman PF, Moore NR, Shepstone BJ: The indeterminate breast mass: Assessment with contrast enhanced magnetic resonance imaging. Br J Radiol, 1994, 67: 14-20.

6. Flickinger FW, Allison JD, Sherry RM, et al: Differentiation of benign from malignant breast masses by time-intensity evaluation of contrast enhanced MRI. Magn Reson Imaging, 1993, 11: 617-620.

7. Harms SE, Flamig DP, Hesley KL, et. al. MR Imaging of the breast with rotating delivery of excitation off resonance: Clinical experience with pathologic correlation. Radiology 187: 493, 1993.

8. Knopp MV, Brix G, Junkermann HJ, Sinn HP: MR mammography with pharmacokinetic mapping for monitoring of breast cancer treatment during neoadjuvant therapy. In Magnetic Resonance Imaging Clinics of North America. Davis PE, Editor. WB Saunders. Nov. 1994, 2 (4): 633-658.

9. Ney FG, Feist JN, Altemus LR, et. al. Characteristic angiographic criteria of malignancy. Radiology 104: 567, 1972.

10. Folkman J, Meerler E, Abernathy C, et. al. Isolation of a tumor factor responsible for angiogenesis. J Exp Med 33:275, 1971.

11. Gilles R; Zafrani B; Guinebretiere JM; Meunier M; Lucidarme O; Tardivon AA; Rochard F; Vanel D; Neuenschwander S; Arriagada R. Ductal carcinoma in situ: MR imaging-histopathologic correlation. Radiology, 1995 Aug, 196(2):415-9.

12. Kaiser WA. MR mammography. Springer-Verlag, Berlin, 1993.

13. Kaiser WA. False-positive results in dynamic MR mammography: Causes, frequency, and methods to avoid. In Magnetic Resonance Imaging Clinics of North America. Davis PE, Editor. WB Saunders. November 1994, 2 (4): 539-556.

14. Brix G, Semmler W, Port G, et al: Pharmacokinetic parameters in CNS Gd-DTPA enhanced MR imaging. J Comp. Assisted Tomog. 15:621, 1991.

15. Mussurakis S; Buckley DL; Bowsley SJ; Carleton PJ; Fox JN; Turnbull LW; Horsman A. Dynamic contrast-enhanced magnetic resonance imaging of the breast combined with pharmacokinetic analysis of gadolinium-DTPA uptake in the diagnosis of local recurrence of early stage breast carcinoma. Investigative Radiology, 1995 Nov, 30(11):650-62.

16. Zuo CS; Jiang A; Buff BL; Mahon TG; Wong TZ. Automatic motion correction for breast MR imaging. Radiology, 1996 Mar, 198(3):903-6.

17. Flanagan FL; Murray JG; Gilligan P; Stack JP; Ennis JT. Digital subtraction in Gd-DTPA enhanced imaging of the breast. Clinical Radiology, 1995 Dec, 50(12):848-54.

18. Boetes C, Barentsz JO, Mus RD. MR characterization of suspicious breast lesions with a gadolinium-enhanced Turbo-FLASH subtraction technique. Radiology 1994; 193: 777-781.

19. Weinreb JC; Newstead G. MR imaging of the breast. Radiology, 1995 Sep, 196(3):593-610.

20. Fobben ES; Rubin CZ; Kalisher L; Dembner AG; Seltzer MH; Santoro EJ. Breast MR imaging with commercially available techniques: radiologic-pathologic correlation. Radiology, 1995 Jul, 196(1):143-52.

21. Dixon WT, Du LN, Faul DD, Gado M, Rossnick S: Projection angiograms of blood labeled by adiabatic fast passage. Magn. Reson. Med., 1986, 3: 454-462.

22. Lee HK, Nalcioglu O, Moran PR: Spatially-resolved flow velocity measurements and projection angiography by selective adiabatic passage. Magn. Reson. Imag., 1991, 9: 115-127.

23. Detre JA, Leigh LS, Williams DS, and Koretsky AP: Perfusion Imaging. Magn. Reson. Med., 1992, 23 (1): 37-45.

24. Walsh EG, Minnematsu K, Leppo J, Moore SC: Radioactive Microsphere Validation of a Volume Localized Continuous Saturation Perfusion Measurement. Magn. Reson. Med., 1994, 31(2): 147-153.

25. Williams DS, Zhang W, Koretsky AP, Adler S: Perfusion imaging of the rat kidney with MR. Radiology, 1994, 190 (3): 813-818.

26. Kwong KK, Chesler DA, Weisskoff RM, Rosen BR. Perfusion MR imaging. Proceedings of Society of Magnetic Resonance, Vol. 2, 1005, (1994).

27. Zhang W, Williams DS, Detre JA, Koretsky AP: Measurement of brain perfusion by volume-localized NMR spectroscopy using inversion of arterial water spins: accounting for transit time and cross-relaxation. Magn. Reson. Med., 1992, 25 (2): 362-371.

28. Pauly J, Le Roux P, Nishimura D, Macovski A. "Parameter relations for the Shinnar-Le Roux selective excitation pulse design algorithm." IEEE Trans. Med. Imaging, 1991, 10(1): 53-65.

29. Zhu DC. Odd-number hybrid echo planar magnetic resonance imaging. Master's thesis. California State University, Sacramento, 1996.

29. Buonocore MH, Zhu DC. Odd-number hybrid EPI. Proceeding of the International Society for Magnetic Resonance in Medicine, 6th Annual Meeting and Exhibition, on CD-ROM, p. 1967 (1998).

31. Jain AK. Fundamentals of Digital Image Processing. Prentice-Hall, Inc., Englewood Cliffs, 1989.

32. Yousem DM, Montone KT, Sheppard LM, Rao VM, Weinstein GS, Hayden RE. "Head and neck neoplasms: magnetization transfer analysis." Radiology, 1994, 192: 703-707.

33. Buonocore MH, Zhu D, Pellot-Barakat C. Measurement of breast tissue perfusion using arterial spin tagging, Proceedings of the International Society for Magnetic Resonance in Medicine 5th Annual Meeting and Exhibition, 1: 311 (1997).

34. Buonocore MH, Zhu DC, Pellot-Barakat C, Zulim RA. Noninvasive measurement of blood flow through breast tumors. Book of Abstracts, California Breast Cancer Research Symposium. Sacramento Convention Center, Sacramento CA, Sept. 16, 1997.

35. Buonocore MH, Zhu DL, Pellot-Barakat C., Zulim RA. Non-invasive measurement of breast tissue perfusion using arterial spin tagging. Radiology, November 1997, 205 (P): 162.

# (9) APPENDIX

***Contributions to Data Analysis***

The regression method derived in this project resolves a key confound that is present in all arterial spin tagging sequences, that of the mismatch of the slice profiles of the inversion and excitation RF pulses. Our sequence is longer than many arterial spin sequences reported in the literature, but we are quite sure that these other methods fail to account for the mismatch, and result in dubious measurements of perfusion. It is interesting to note that the mismatch results in signal contamination who spatial dependence resembles an inverted $T_1$ weighted image, thus, they are easily mistaken for true perfusion maps (i.e. in the brain, CSF is bright, followed by gray matter, then white matter, just as true perfusion would present).

Derivation of semi-log linear regression method

In this derivation, it is assumed that, because the excitation RF flip angle is small, repeated application of these pulses for data acquisition does not disturb $T_1$ recovery of the inverted spins, nor the equilibrium magnetization of the imaged spins if not inverted. Given this assumption, under a spin tagging condition, the steady-state longitudinal magnetization at the end of each $TR$ period just before the next inversion pulse would be

$$M_{t0ss} = M_0\,(1-e^{-b\,TR}) - M_{t0ss}\,e^{-b\,TR}$$

where, $M_{t0ss}$ = the steady-state longitudinal magnetization at the end of each $TR$ period, $M_0$ = the longitudinal magnetization under fully relax condition, $TR$ = the repetition time, and

$$b = \begin{cases} \dfrac{1}{T_{1s}} & \text{for the Selective Tagging Condition} \\ \dfrac{1}{T_{1n}} & \text{for the Non-selective Tagging Condition} \end{cases}$$

Therefore,

$$M_{t0ss} = M_0 \frac{1-e^{-b\,TR}}{1+e^{-b\,TR}} \qquad \text{(A.1)}$$

The longitudinal magnetization at time $t$ after the spin inversion at steady-state is

$$M_t(t) = M_0(1-e^{-bt}) - M_{t0ss}e^{-bt} \tag{A.2}$$
$$= M_0(1-e^{-bt}) - M_0\frac{1-e^{-bTR}}{1+e^{-bTR}}e^{-bt}$$
$$= M_0(1-e^{-bt} - \frac{1-e^{-bTR}}{1+e^{-bTR}}e^{-bt})$$
$$= M_0(1-\frac{2e^{-bt}}{1+e^{-bTR}})$$

As a result, the signal measured at echo time *TE* is

$$S_t = M_0(1-\frac{2e^{-bTI}}{1+e^{-bTR}})\sin(\theta)e^{-\frac{TE}{T2}} \tag{A.3}$$

where, *TI* = the time of inversion from the inversion pulse to the effective center of k space, T*E* = the time of echo at each read-out period, and $\theta$ = the excitation flip angle.

Under the Regular Tagging Condition, the longitudinal magnetization $M_{reg}(t)$ at any time *t* stays at equilibrium. Specifically,

$$M_{reg}(t) = M_0 \tag{A.4}$$

The signal measured at echo time *TE* becomes

$$S_{reg} = M_0\sin(\theta)e^{-\frac{TE}{T2}} \tag{A.5}$$

Thus,

$$\frac{S_t}{S_{reg}} = 1-\frac{2e^{-bTI}}{1+e^{-bTR}} \tag{A.6}$$

and,

$$1-\frac{S_t}{S_{reg}} = \frac{2e^{-bTI}}{1+e^{-bTR}}$$

Thus, considering the *i*th inversion time (TI):

$$\frac{S_{reg}-S_t(i)}{S_{reg}-S_t(j)} = \frac{e^{-bTI(i)}}{e^{-bTI(j)}} \tag{A.7}$$
$$= e^{-b(TI(i)-TI(j))}$$

where, *TI*(*i*) = the time of inversion at the *i*th *TI* cycle, $S_t(i)$ = the signal at a pixel when *TI*(*i*) is used, *TI*(*j*) = the time of inversion at the *j*th *TI* cycle, $S_t(j)$ = the signal at a pixel when *TI*(*j*) is used. Taking the logarithm of both sides yields,

$$\ln(S_{reg} - S_t(i)) - \ln(S_{reg} - S_t(j)) = -b(TI(i) - TI(j))$$

and solving for $b$ gives,

$$b = -\frac{\ln(S_{reg} - S_t(i)) - \ln(S_{reg} - S_t(j))}{TI(i) - TI(j)} \qquad \text{(A.8)}$$

The above equation shows the semi-log linear regression relationship between ($S_{reg}$ - $S_t$) and $TI$. The formula can be applied to both Selective and Non-selective tagging conditions, do derive $b_s$ and $b_n$, respectively. The exact values of the effective $TI$'s are uncertain (due data collection is spread out over 1 second). Nevertheless, it is reasonable to assume that these values each have the same amount of time error relative to their true values. Because $TI(i)$ and $TI(j)$ is subtracted in the denominator, the uncertainty of the timing of this "effective" $TI$ cancels out.

Elimination of slice profile mismatch effects

The semi-log relationship eliminates the errors due to mismatch between the slice profiles of the inversion and data acquisition RF pulses. Because the RF pulses used for inversion and data acquisition are different under the Selective Condition, (The Non-selective Condition does not have this problem because the RF inversion pulse inverts spins everywhere.).

The geometric mismatch between the inversion and read-out profiles would lead to the contamination of signal from non-inverted spins. Thus the apparent signal from the Selective Condition can be modeled as

$$S_{sel_{app}} = (1 - err)S_{sel} + err\ S_{reg} \qquad \text{(A.9)}$$

where $S_{sel}$ = the signal of a pixel if no slice profile mismatch, $S_{sel_{app}}$ = the signal of a pixel actually measured, and $err$ = the amount of percent error due to slice profile mismatch. Then,

$$\frac{S_{sel_{app}}}{S_{reg}} = (1 - err)\frac{S_{sel}}{S_{reg}} + err$$

and

$$\frac{S_{sel}}{S_{reg}} = \frac{\frac{S_{sel_{app}}}{S_{reg}} - err}{1 - err}$$

Thus,

$$\frac{S_{reg}-S_{sel}}{S_{reg}}=\frac{1-err-\frac{S_{sel_{app}}}{S_{reg}}+err}{1-err} \qquad (A.10)$$

$$=\frac{1-\frac{S_{sel_{app}}}{S_{reg}}}{1-err}$$

Comparing with Eq. (A.7), we have

$$\frac{S_{reg}-S_{sel_{app}}(i)}{S_{reg}-S_{sel_{app}}(j)}=e^{-b_s\,(TI(i)-TI(j))}$$

where,

$b_s=\frac{1}{T_{1s}}=\frac{1}{T_1}+\frac{f}{\lambda}$ = the $b$ value under the Selective Condition

Thus,

$$b_s=\frac{\ln(S_{reg}-S_{sel_{app}}(i))-\ln(S_{reg}-S_{sel_{app}}(j))}{TI(i)-TI(j)} \qquad (A.11)$$

Eq. (A.11) corresponds exactly as Eq. (A.8). In other words, by using the semi-log linear regression method, the problem due to geometric mismatch between the inversion and read-out slice profiles is eliminated.

***Phantom, normal subject, and patient study notes***

These notes (pages 41-50, presented in two-column landscape mode) were written immediately after each study, and provide brief subject history, and detailed listing of pulse sequences and parameters used in the protocol, and problems noted. Preliminary accounts of studies prior to 11/19/97 have been reported [33,34,35].

**Inventory of Breast Imaging Studies to Date**

| | Test Phantoms | Normal Subject | Patient (no CE-MRI) No biopsy | Patient (no CE-MRI) Biopsy | Patient (with CE-MRI) Biopsy |
|---|---|---|---|---|---|
| Prior to 10/1/98 | 9 | 4 | 3 | 3b, 2m | 0 |
| Since 10/1/98 | 5 | 1 | 1 | 4b | 2b |

CE-MRI (dynamic first-pass contrast-enhanced MRI). Number preceding **b** indicates number of subjects in which the biopsy revealed benign disease. Number preceding **m** indicates number of subjects in which the biopsy revealed malignant disease. Patients without biopsy did not meet clinical criteria and mass was assumed benign.

Subject Study Summary:

Study Descriptions: February 2, 1997 through August 8, 1998

(Procedure Updated on 2/7/97)
Date of study: 2/7/97

Breast Sequence Study
by Michael Buonocore and David Zhu

Patient: Neva (NORMAL SUBJECT)

Suggest procedures:

1. 2D Spin Echo axial cut (Series 1), TR = 600 ms, 1 acquisition

2. 2D fast spin echo (Series 2)
TE2=128 msec, TE=17 msec, TR=4s,
5mm with 1 mm interslice, , Center:
Increases to 20 slices

3. 3D scan coronal cut (Series 3):
Location:

4. David's breast sequence coronal cut: fgt1_new

Five TI cycles, br_TR = 2.7 s, br_TI = 15 ms, ti_inc = 150 ms.
TI decreases from 615 ms to 15 ms.

Slice thickness: 3 mm
Frequency direction: R/L for all locations
Prescan: R1 =6 , R2 = 15, TG =169 or 167

series 4: location: p20
series 5: location: p15
series 6: location: a0
series 7: location: a22
series 8: location: a30
series 9: location: a40
series 10: location: a50

5. Redo 3D scan coronal cut (series 11), type: SPGR PROSP

(Procedure Updated on 2/7/97)
Date of study: 3/2/97

Flow Phantom Study
by David Zhu

Coil: breast coil

Suggest procedures:

David's breast sequence axial cut: fgt1_new

Five TI cycles, opfphases = 55, br_TR = 2.7 s, br_TI = 15 ms,
ti_inc = 150 ms, TI decreases from 615 ms to 15 ms.

Slice thickness: 3 mm
br_sel_sl = opslthick = 3mm

Frequency direction: R/L

phantom on the left of the breast coil in prone.

Location: A30



| | Flow rate: | | Motor mark |
|---|---|---|---|
| series 1: | Motor off | | R1 = 6, R2 =15, TG =107 |
| series 2: | 40 ml /91.93 sec | 0.5 | TG = 112 |
| series 3: | 100 ml /79.62 sec | 0.8 | TG = 114 |
| series 4: | 80 ml / 96.47 sec | 0.66 | TG = 123 |
| series 5: | 100 ml / 64.68 sec | 0.9 | TG = 115 |
| series 6: 100 ml /54.46 sec | | 1.0 | TG = 123 |

ia_rf1: current val: 1163
ia_rf0: current val: 32767
ia_gzrf1: current val: 32071
ia_gzrf0: current val: 25657
ratio_rf0_1_ext: current val: 28.16
ratio_rf0_1_full: current val: 2.914
ti_inc: The increment of TI current val: 150000
yhybrid: current val: 1 min: -2147483647 max: 2147483647 type: Integer

Date of study: 3/5/97

Head study using Breast Sequence
by Michael Buonocore and David Zhu

Subject: Marijana (Fibroadenoma)

Local Coil (lgc)
Supine, nasion, fov = 22cm, cfxfull, cfyfull and cfzfull are scaled down.

Procedures:

1. 2D Spin Echo coronal cut (Series 1)

2. David's breast sequence coronal cut: fgt1_new

Five TI cycles, br_TR = 2.7 s, br_TI = 15 ms, ti_inc = 150 ms.
TI decreases from 615 ms to 15 ms.

Acquisitoin slice thickness: 3 mm
Selective slice thikness: 3mm
Frequency direction: S/I for all locations
Prescan: R1 = 6 , R2 = 15 , TG = 113

FOV: 22 cm

series 2: location: P24
series 3: location: P16
series 4: location: A0

optr = 16444
opte = 9244

Date of study: 3/5/97

Breast Sequence Study
by Michael Buonocore and David Zhu

Subject: Marijana (Fibroadenoma)

Procedures:

1. 2D Spin Echo axial cut (Series 1)

2. 2D fast spin echo (Series 2)

3. 3D scan coronal cut (Series 3): Patsat needed to add

4. David's breast sequence coronal cut: fgt1_new

Five TI cycles, br_TR = 2.7 s, br_TI = 15 ms, ti_inc = 150 ms.
TI decreases from 615 ms to 15 ms.

Acquisitoin slice thickness: 3 mm
Selective slice thickness: 3mm
Frequency direction: R/L for all locations
Prescan: R1 =6, R2 = 15, TG = 177

series 4: location: A30
series 5: location: A33
series 7: Repeat series 5 with the same locatoin, but with a br_TI = 50 ms, so TI decrease from 650 ms to 50 ms
series 8: location: A36

---

Date of study: 5/3/97

Breast Sequence Study
by Michael Buonocore and David Zhu

Patient: Nancy Saunders

Procedures:

1. 2D Spin Echo axial cut (Series 1)

2. 2D fast spin echo (Series 2)

3. 3D scan coronal cut (Series 3): Fatsat is added,
P26.8 to A108.9
Scan thickness: 2.3 mm

4. David's breast sequence coronal cut: fgt1_new

Five TI cycles, br_TR = 2.7 s, br_TI = 15 ms, ti_inc = 150 ms.
TI decreases from 615 ms to 15 ms.

Acqluisitoin slice thickness: 3 mm
Selective slice thikness: 3mm
Frequency direction: R/L for all locations
Prescan: R1 = 6 , R2 = 15 , TG = 180 (autoprescan fails with the limit of TG at 172, manuely set 180)

series 4: location: A23.8
series 5: location: A21.5
series 6: location: A85.9
series 7: location: A88.2

comments:
Suspected of fibroadenoma.
Two cysts or tumors at left breast.
Autoprescan fails with the limit of TG at 172, manuely set 180.

Question: Is inversion set at optimal 180 degree? How to take care of the non-optimal inversion pulse?

---

Date of study: 5/11/1997 (May 11, 97)

Phantom study

---

Date of study: 5/17/97

breast sequence study

7up phantom

A30, R/L freq

40 cm FOV

(1) fgt1_new3:

R1=6, R2 = 15, TG = 109

(2) fgt1_new1

R1 = 6, R2 = 15, TG = 113

---

Date of study: 5/23/97

Breast Sequence Study
by Michael Buonocore and David Zhu

Patient Name: Jean (86 years old) (TUMOR RIGHT BREAST)

Procedures:

1. 2D Spin Echo axial cut (Series 1)

2. 2D fast spin echo (Series 2)

3. 3D scan coronal cut (Series 3):

P13.3 to A 51.5

Scan thickness: 2.4 mm,
# of scan loc: 28

4. David's breast sequence coronal cut: fgt1_new3

Five TI cycles, br_TR = 2.7 s, br_TI = 15 ms, ti_inc = 150 ms.
TI decreases from 615 ms to 15 ms.

Acquisition slice thickness: 3 mm
Selective slice thickness: 3mm
Frequency direction: R/L for all locations
Prescan: R1 = 6 , R2 = 15 , TG = 146

series 4: location: A15.5
series 5: location: A20
series 6: location: A26
series 7: location: A32
series 8: location: A38

comments: Tumor locates at right breast

---

Date of study: 5/24/97

Breast Sequence Study
by Michael Buonocore and David Zhu

Patient Name: Quan (David's mother-in-law)(NORMAL SUBJECT)
age: 55

Procedures:

1. 2D Spin Echo axial cut (Series 1): TE = minimum, TR = 600 ms

2. 2D fast spin echo (Series 2): p60 - a66

3. 3D scan coronal cut (Series 3):

P 22.9 to A 68.9

Scan thickness: 3.4 mm

4. David's breast sequence coronal cut: fgt1_new3

Five TI cycles, br_TR = 2.7 s, br_TI = 15 ms, ti_inc = 150 ms.
TI decreases from 615 ms to 15 ms.

Acquisitoin slice thickness: 3 mm
Selective slice thikness: 3mm
Frequency direction: R/L for all locations
Prescan: R1 = 6 , R2 = 15 , TG = 179

series 4: location: P 2.5
series 5: location: A 17.9
series 6: location: P 5.9
series 7: location: A 28.1
series 8: location: A 48.5
series 9: location: A55.3 (redo prescan: R1 = 6, R2 = 15, TG = 171)

comments: Normal subject

---

Date of study: 7/6/97

Head study
by David Zhu

Subject: Grandma
Age: 81
Complains: headache at top of head. Pressing palm over head can reduce headache.
Headache can relocate to other area of the head.

Procedure: Use Spin Echo (Brain Screen),
TE = 80 ms, TR = 2 s (heavy T2-weighting)
256 x 192
slice thickness: 5 cm
interslice space: 2.5 cm

(1) Saggital (series 1)

# of slice: 12
Location: L40, R42.5

(2) Axial (series 2)

# of slice: 17
Location: s85, i57.5

(3) Coronal (series 3)

# of slice: 19
Location: a45, p90

(4) 3D, coronal, 256 x 128 (series 4)

20 degree flip angle
TE: minimum
TR: 50 msec
Thickness: 1.5 mm
# of scan loc: 28

---

Date of study: 7/6/97

Test sequence: fg_1p6.e

To check whether we can run fgre using opslthick of 1.7 mm.

Result:

(1) opslthick = 1.7 mm, bw_rf1 = 700 Hz, opflip = 20

I.1 to I.5

Autoprescan successful: R1 = 6, R2 = 15, TG = 68
Scan successful.

(1) opslthick = 3 mm, bw_rf1 = 1250 Hz, opflip = 20

I.6 to I.10

Autoprescan successful: R1 = 6, R2 = 15, TG = 68
Scan successful. These regular images appear to be darker than those
with opslthick of 1.7 mm.

---

Date of study: 7/11/97

Breast Sequence Study
by Michael Buonocore and David Zhu

Patient Name: Breast biopsy patient (MISSED TUMOR NEXT TO NIPPLE, OTHERWISE NORMAL)

age: about 60

Procedures:

1. 2D Spin Echo axial cut (Series 1): I30 to S30

2. 2D fast spin echo (Series 2)

3. 3D scan coronal cut (Series 3):

P 11.2 to A 69.8

Scan thickness: 5 mm

4. David's breast sequence coronal cut: fgt1_new3b

Five TI cycles, br_TR = 2.7 s, br_TI = 15 ms, ti_inc = 150 ms.
TI decreases from 615 ms to 15 ms.

Acquisition slice thickness: 3 mm
Selective slice thickness: 3mm
Frequency direction: R/L for all locations
Prescan: R1 = , R2 = , TG =

series 4: location:A27.8, R1 = 4, R2 = 14, TG - 170 (might not be good)
series 5: location: A2, R1 = 6, R2 - 15, TG 179
series 6: location: A21
series 7: location: A30

comments: Tumor locates at right breast, about 3 o'clock near nipple, not biopsy yet.
We might have missed it. (Correct, did not scan at correct location)

---

Date of study: 7/26/97

7-up phantom testing

001: fgt1_new3b, default setting
autoprescan: R1 = 6, R2 =15, TG = 109

001: fgt1_new3c, default setting
autoprescan: R1 = 6, R2 =15, TG = 107

Date of study: 7/26/97

Breast Sequence Study
by David Zhu

Patient Name: Grandma (NORMAL)
age: 81

Procedures:

1. 2D Spin Echo axial cut (Series 1)

2. 3D scan coronal cut (Series 3):

P 21.4 to A 59.6

Scan thickness: 3 mm

4. David's breast sequence coronal cut: fgt1_new3c

Seven TI cycles, br_TR = 2.7 s, br_TI = 15 ms, ti_inc = 100 ms.
TI decreases from 615 ms to 15 ms.

Acquisition slice thickness: 3 mm
Selective slice thickness: 3mm
Frequency direction: R/L for all locations
Prescan: R1 = 6 , R2 = 15 , TG = 178

series 3: location: A8.6
series 4: location: A23.6
series 5: location: A35.6
series 6: location: A44.6

comments: Subject did not complain of any abnormality.

Date of study: 8/1/97:

Flow phantom study using fgt1_new3c:

| Series Number | Flow Mark |
|---|---|
| 001 | 0 |
| 002 | 0.5 |
| 003 | 0.8 |
| 004 | 1.0 |

Date of study: 8/6/97

Breast Sequence Study
by Michael Buonocore and David Zhu

Patient Name: Josie (SIGNET CELL CARCINOMA)
age: 44

Procedures:

1. 2D Spin Echo axial cut (Series 1)

2. 2D fast spin echo (Series 2) P30 - A60

3. 3D scan coronal cut (Series 3):

P 2.9 to A 64.6

Scan thickness: 2.5 mm

4. 3D scan coronal cut (Series 4):

whole breast

Scan thickness: 3.7 mm

5. Redo No. 2 due to patient movement. (Series 5)

6. David's breast sequence coronal cut: fgt1_new3c

Seven TI cycles, br_TR = 2.7 s, br_TI = 15 ms, ti_inc = 100 ms.
TI decreases from 615 ms to 15 ms.

Acquisitoin slice thickness: 3 mm
Selective slice thikness: 3mm
Frequency direction: R/L for all locations
Prescan: R1 = 6 , R2 = 15 , TG = 153

series 6: location: A14
series 7: location: A24
series 8: location: A30

comments:
Tumors are at right breast from various locations.
One big biopsy site at inner bottom of the right breast.
Probably cancer patient.

Aug 9, 1997: Meat phantom
Date of study: 8/9/97

Breast Sequence Study
by David Zhu

Phantom study (meat phantom always on left, prone position)

Procedures:

Place only the Meat phantom.

1. 2D Spin Echo axial cut (Series 1) : i30 to s30, 11 locs, thick: 5, inter: 1
R1 = 6 , R2 = 15 , TG = 75

2. 2D fast spin echo (Series 2) : thick:5, inter:1, a20-a60, 8 locs.
R1 = 6 , R2 = 15 , TG = 75

3. 3D scan coronal cut (Series 3):

P 19.2 to A 59.7

Scan thickness: 1.5 mm
No of loc: 28
R1 = 6 , R2 = 15 , TG = 76

4. David's breast sequence coronal cut: fgt1_new3c

Seven TI cycles, br_TR = 2.7 s, br_TI = 15 ms, ti_inc = 100 ms.
TI decreases from 615 ms to 15 ms.

Acquisitoin slice thickness: 3 mm
Selective slice thikness: 3mm
Frequency direction: R/L for all locations

series 4: location: a20 , R1 = 6 , R2 = 15 , TG = 116
series 5: location: a38 , R1 = 6 , R2 = 15 , TG = 115
series 6: location: a50, R1 = 6 , R2 = 15 , TG = 116

Place the Meat phantom with the get phantom

series 7: location: a38, R1 = 6 , R2 = 15 , TG = 106

Place the Meat phantom with the 7-up phantom

series 8: location: a38 R1 = 6 , R2 = 15 , TG = 111

Purpose:

(1) Check perfusion with meat with no blood flowing.

(2) Observe how the prescan result changes with the placement of differnt tissue type.

---

Aug 30, 1997
Date of study: 8/30/97

Breast Sequence Study
David Zhu

Subject Name: Tracy
age: 19

Procedures:

1. 2D Spin Echo axial cut (Series 1)
I 84 - s84, loc: 29. Scan thick = 5 mm, Inter = 1 mm.

2. 2D fast spin echo (Series 2)
P10 -> A56. Scanthick = 5 mm, inter = 1mm

3. 3D scan coronal cut (Series 3):

P 2.3 to A 49.2

Scan thickness: 2 mm

4. David's breast sequence coronal cut: fgt1_new3c

Seven TI cycles, br_TR = 2.7 s, br_TI = 15 ms, ti_inc = 100 ms.
TI decreases from 615 ms to 15 ms.

Acquisition slice thickness: 3 mm
Selective slice thickness: 3mm
Frequency direction: R/L for all locations
Prescan: R1 = , R2 = , TG =

series 4: location: A2 R1 = 6 , R2 = 15 , TG = 140

series 5: location: A7 R1 = 6 , R2 = 15, TG = 139
series 6: location: A10 R1 = 6 , R2 = 15, TG = 140
series 7: location: A14 R1 = 6 , R2 = 15 , TG = 145
series 8: location: A20 R1 = 6 , R2 = 15, TG = 148
series 9: location: A32 R1 = 6 , R2 = 15 , TG = 141
Series 10: repeat No. 2 (2d fse).
P15 - A21, scan thick = 3 mm, inter = 1mm.

comments:
Normal healthy subject, 10 monthes after giving birth.
Subject complains that she has a mass on both breasts above nipple; the masses are harder than other tissues; they are about 2 cm in diameter; they have been there for 4 to 5 years; the size did not change.

---

Sep 13a, 97
Date of study: 9/13/97

Breast Sequence Study
David Zhu

Subject Name: Tracy
age: 19

Redo Study of 8/30/97

Ask subject to have a better fit of the foam cast, tighter strap, and not to move, and to breath smoothly with stomach.

Procedures:

1. 2D Spin Echo axial cut (Series 1)
I 60 - s 60, loc: 21 . Scan thick = 5 mm, Inter = 1 mm.

2. 2D fast spin echo (Series 2)

P2 - A58, loc: 16, scan thick = 3 mm, inter = 1mm.

4. David's breast sequence coronal cut: fgt1_new3c

Seven TI cycles, br_TR = 2.7 s, br_TI = 15 ms, ti_inc = 100 ms.
TI decreases from 615 ms to 15 ms.

Acquisitoin slice thickness: 3 mm
Selective slice thikness: 3mm
Frequency direction: R/L for all locations
Prescan: R1 = , R2 = , TG =

series 3: location: A6 R1 = 6, R2 = 15 , TG =138
series 4: location: A10 R1 = 6 , R2 = 15 , TG = 139
series 5: location: A14 R1 = , R2 = , TG =
series 6: location: A18 R1 = 6 , R2 =15 , TG =137
series 7: location: A22 R1 = , R2 = , TG =
series 8: location: A26 R1 = 6 , R2 = 15 , TG = 138
series 9: location: A34 R1 = 6 , R2 =15 , TG =137

comments:
Normal healthy subject, 10 monthes after giving birth.
Subject complains that she has a mass on both breasts above nipple; the masses are harder than other tissues; they are about 2 cm in diameter; they have been there for 4 to 5 years; the size did not change. Sometimes there is slight pulling kind of pain.

The motion-resist procedure shows to be effective based on the data acquired.

---

Sep 13b, 1997
9/13/97

Study with 7-up bottles at location A = 0. See if the calcuated T1n and f/lambda different at lower locations.

Sequence: fgt1_new3c

---

9/20/97, (Sep 20, 97)

Meat phantom experiment using fgt1_new3c to check the image quality close to chest wall.
Sequence: fgt1_new3c

---

Sep 27, 97
9/27/97
Sat

7-up phantom study
by David Zhu

series 001:
Number of images = 10, br_norm = 2, br_tino = 2, br_acqs = 2,
br_TI = 100 ms, ti_inc = 200 ms, br_TR = 2.7 s
FOV = 34 cm

(1) I.001 - I.010: fgt1_new3d, set 256 x 128, others default
(2) I.011 - I.020: Addition to (1), set rhrcyres = 128.
(3) I.021 - I.030: Addition to (2), set rhphasescale = 0.5.
(4) I.031 - I.040: Addition to (3), set phasefov = 128.
(5) I.041 - I.050: fgt1_new3d, 256 x 256

series 002:
fgt1_new3c, default to 61 images, and fov 34 cm
series 003:
fgt1_new3d, default to 61 images as in fgt1_new3c, but set 256 x 128, and set rhrcyres = 128, rhphasescale = 0.5, phasefov = 128.

Purpose of study: See if fgt1_new3d better. It offers better resolution.

---

Date of study: 10/4/97

Different phantom study by David Zhu

(1) comparing fgt1_new3c with fgt1_new3d
(2) Crude flow phantom study.
(3) Orientation of the object and image study.

---

Date of Study: Oct 11, 97

10/11/97
flow phantom study
by David Zhu

Test sequence fgt1_new3d
FOV = 34

series 001: axial cut using spin echo

The following has FOV = 34 and A24
fgt1_new3d, default setting

| series | pump mark flow | measurement |
|---|---|---|
| 002 | 0 | ---- |
| 003 | 0.5 | 40 ml/1'18" |
| 004 | 0.66 | 100 ml/1'46" |
| 005 | 0.8 | 100 ml/1'14" |
| 006 | 0.9 | 100 ml/1'02" |
| 007 | 1.0 | 120 ml/1'03" |
| 008 | 1.1 | 140 ml/1'07" |

---

Date of study: 10/12/97
Breast Sequence Study
Michael Buonocore and David Zhu

Subject Name: Joy Watts
age: 72

Ask subject to have a better fit of the foam cast, tighter strap,
and not to move, and to breath smoothly with stomach.

Procedures:

1. 2D Spin Echo axial cut (axial)
I 84 - s 84 , loc: 29 . Scan thick = mm, Inter = mm.

2. 2D fast spin echo (Series 1)
P 24 - A 60 , loc: 30 , scan thick = mm, inter = mm.

3. David's breast sequence coronal cut: fgt1_new3d, fov = 34

Seven TI cycles, br_TR = 2.7 s, br_TI = 15 ms, ti_inc = 100 ms.
TI decreases from 615 ms to 15 ms.

Acquisitoin slice thickness: 3 mm
Selective slice thikness: 3mm
Frequency direction: R/L for all locations
Prescan: R1 = , R2 = , TG =

series 2: location: a18 R1 = 6 , R2 = 15 , TG = 165

series 3: location: a0 R1 = , R2 = , TG =
series 4: location: a46 R1 = 6 , R2 = 15 , TG = 183
series 5: location: a12 R1 = 6 , R2 = 15 , TG = 161
series 6: location: a42 R1 = 6 , R2 = 15 , TG = 183
series 7: location: a30 R1 = 6 , R2 = 15 , TG = 172
series 8: location: a48 R1 = 6 , R2 = 15 , TG = 184
series 9: location: a24 R1 = 6 , R2 = 15 , TG = 171
series 10: location: a36 R1 = 6 , R2 = 15 , TG = 174
series 11: location: a51 R1 =6 , R2 = 15 , TG = 190
series 12: location: a54 R1 = 6 , R2 = 15, TG = 191

comments:
The tumor is at the right breast above the nipple.

---

(Procedure Updated on 11/15/97)
Date of study: 11/15/97
Breast Sequence Study
by Michael Buonocore and David Zhu

Type of study: phantom( ), Normal subject ( ), Patient (x)

Name: Silvia Smart Age: 42

Preparation:
Ask subject to have a better fit of the foam cast, tighter strap,
and not to move, and to breath smoothly with stomach.

Procedures:

1. 2D Spin Echo axial cut (Series 1) FOV = 40

I 84 to s 84 , loc: 29 . Scan thick = mm, Inter = mm.

2. 2D Fast Spin Echo (Series 2) FOV = 34

P 22 to A 80 , loc: 19 , scan thick = 5 mm, inter = 1 mm.

3. David's breast sequence coronal cut: fgt1_new3d, fov = 34

Seven TI cycles: br_TR = 2.7 s, br_TI = 15 ms, ti_inc = 100 ms.
TI decreases from 615 ms to 15 ms.
Acquisitoin slice thickness: 3 mm, Selective slice thikness: 3mm
Frequency direction: R/L for all locations

series 3: location:A18 R1 = 5 , R2 = 14 , TG = 185
series 4: location:A23 R1 = 5 , R2 = 14 , TG = 185
series 5: location:A13 R1 = 6 , R2 = 15 , TG = 185
series 6: location:A8 R1 = 6 , R2 = 15 , TG = 185
series 7: location:A28 R1 = 6 , R2 = 15 , TG = 185
series 8: location:A3 R1 = 6 , R2 = 15 , TG = 185
series 9: location:A33 R1 = 6 , R2 = 15 , TG = 185
series 10: location:P2 R1 = 6 , R2 = 15 , TG = 185
series 11: location:A38 R1 = 6 , R2 = 15 , TG = 185

series 12: location:P7 R1 = 6 , R2 = 15 , TG = 185

Comments:
Tumor locates at left breast, 6 o'clock, about 1/3 in from the nipple.

Prescan cannot set TG, mannually set TG to 185 for all.
R1 = 5 and R2 = 14 seem to be too low. Manually set most prescan to
R1 = 6 and R2 = 15. Hope R1 = 5 and R2 = 14 do not have problem.

---

(Procedure Updated on 11/15/97)
Date of study: 11/16/97
Breast Sequence Study
by Michael Buonocore and David Zhu

Type of study: phantom( ), subject ( x), Patient ( )

Name: Kim Buonocore Age: 38

Preparation:
Ask subject to have a better fit of the foam cast, tighter strap,
and not to move, and to breath smoothly with stomach.

Procedures:

1. 2D Spin Echo axial cut (Series 1) FOV = 40

I 84 to s 84 , loc: 29 . Scan thick = 5 mm, Inter = 1 mm.

2. 2D Fast Spin Echo (Series 2) FOV = 34

P 7 to A 55 , loc: 12 , scan thick = 5 mm, inter = 1 mm.

3. David's breast sequence coronal cut: fgtl_new3d, fov = 34

Seven TI cycles: br_TR = 2.7 s, br_TI = 15 ms, ti_inc = 100 ms.
TI decreases from 615 ms to 15 ms.
Acquisitoin slice thickness: 3 mm, Selective slice thikness: 3mm
Frequency direction: R/L for all locations

series 3: location:P7 R1 = 6 , R2 = 15 , TG = 153
series 4: location:P1 R1 = 6 , R2 = 15 , TG = 154
series 5: location:A5 R1 = 6 , R2 = 15 , TG = 153
series 6: location:A11 R1 = 6 , R2 = 15 , TG = 154
series 7: location:A17 R1 = 6 , R2 = 15 , TG = 160
series 8: location:A23 R1 = 6 , R2 = 15 , TG = 160
series 9: location:A29 R1 = 6 , R2 = 15 , TG = 160
series 10: location:A35 R1 = 6 , R2 = 15 , TG = 167

Comments:
Fibroadenoma is at left breast, about 1/3 in from nipple, about 3 o'clock position.

---

(Procedure Updated on 11/19/97)
Date of study: 11/19/97
Breast Sequence Study
by Michael Buonocore and David Zhu

Type of study:phantom( ), normal subject ( ), subject w/ suspecious lesion (x)

Name: Leslie Decard Age: 55

Preparation:
Ask subject to have a better fit of the foam cast, tighter strap,
and not to move, and to breath smoothly with stomach.

Procedures:

1. 2D Spin Echo axial cut (Series 1) FOV = 40

I 84 to s 84 , loc: . Scan thick = 5 mm, Inter = 1 mm.

2. 2D Fast Spin Echo (Series 2) FOV = 34

P to A , loc: , scan thick = 5 mm, inter = 1 mm.

3. David's breast sequence coronal cut: fgtl_new3d, fov = 34

Seven TI cycles: br_TR = 2.7 s, br_TI = 15 ms, ti_inc = 100 ms.
TI decreases from 615 ms to 15 ms.
Acquisitoin slice thickness: 3 mm, Selective slice thikness: 3mm
Frequency direction: R/L for all locations

series 3: location: A16 R1 = 6 , R2 = 15 , TG = 162, I32
series 4: location: A10 R1 = 6 , R2 = 15 , TG = 167, I32
series 5: location: A4 R1 = 6 , R2 = 15 , TG = 170, I10
series 6: location: P2 R1 = 6 , R2 = 15 , TG = 168, I10
series 7: location: P8 R1 = 6 , R2 = 15 , TG = 163, I10
series 8: location: P14R1 = 6 , R2 = 15 , TG = 162, I10
series 9: location: P20R1 = 6 , R2 = 15 , TG = 161, I10
series 10: location: P26,R1 = 6 , R2 = 15 , TG = 164, I10
series 11: location: A22,R1 = 6 , R2 = 15 , TG = 169, I10
series 12: location: A19, R1 = 6 , R2 = 15 , TG = 165, I10

Comments:
Tumor at left breast, close to checst wall, lateral.

---

(Procedure Updated on 11/19/97)
Date of study: 12/10/97
Breast Sequence Study
by Michael Buonocore and David Zhu

Type of study:phantom( ), normal subject ( ), subject w/ suspecious lesion (x)

Name: Lorraine Age: ~ 68

Preparation:
Ask subject to have a better fit of the foam cast, tighter strap,
and not to move, and to breath smoothly with stomach.

Procedures:

1. 2D Spin Echo axial cut (Series 1) FOV = 40

I 84 to s 84 , loc: 29 . Scan thick = mm, Inter = mm.

2. 2D Fast Spin Echo (Series 2) FOV = 34

P 14 to A 94 , loc: 19 , scan thick = mm, inter = mm.

3. David's breast sequence coronal cut: fgtl_new3d, fov = 34

Seven TI cycles: br_TR = 2.7 s, br_TI = 15 ms, ti_inc = 100 ms.
TI decreases from 615 ms to 15 ms.
Acquisitoin slice thickness: 3 mm, Selective slice thikness: 3mm
Frequency direction: R/L for all locations

series 3: location: A0 R1 =6 , R2 = 15 , TG = 159
series 4: location:A4 R1 = , R2 = , TG =
series 5: location:A10 R1 = 6 , R2 =15 , TG = 160
series 6: location:A13 R1 = , R2 = , TG =
series 7: location:A16 R1 = 6 , R2 = 15 , TG = 160
series 8: location:A19 R1 = , R2 = , TG =
series 9: location:A22 R1 = , R2 = , TG =
series 10: location:A28 R1 = 6 , R2 = 15 , TG = 160
series 11: location:A34 R1 = , R2 = , TG =
series 12: location:A40 R1 = 6 , R2 = 15 , TG = 161

Comments: Tumor at left breast, 9 o'clock.

Procedure Updated on 11/19/97)
Date of study: 12/14/97
Breast Sequence Study
by Michael Buonocore and David Zhu

Type of study:phantom( ), normal subject (x), subject w/ suspecious lesion ( )

Name: Anti Fu Age: about 40

Preparation:
Ask subject to have a better fit of the foam cast, tighter strap,
and not to move, and to breath smoothly with stomach.

Procedures:

1. 2D Spin Echo axial cut (Series 1) FOV = 40

I 84 to s 84 , loc: 29 . Scan thick = 5 mm, Inter = 1 mm.

2. 2D Fast Spin Echo (Series 2) FOV = 34

P 22 to A 36 , loc: 11 , scan thick = 5 mm, inter = 1 mm.

3. David's breast sequence coronal cut: fgt1_new3d, fov = 34

Seven TI cycles: br_TR = 2.7 s, br_TI = 15 ms, ti_inc = 100 ms.
TI decreases from 615 ms to 15 ms.
Acquisitoin slice thickness: 3 mm, Selective slice thikness: 3mm
Frequency direction: R/L for all locations

series 3: location:P22 R1 = 6 , R2 =15 , TG = 187
series 4: location:P16 R1 = , R2 = , TG =
series 5: location:P10 R1 = 6 , R2 = 15 , TG =188
series 6: location:P4 R1 = , R2 = , TG =
series 7: location:A2 R1 = 6 , R2 = 15 , TG = 192
series 8: location:A8 R1 = 6 , R2 = 15 , TG = 194
series 9: location:A14 R1 = , R2 = , TG =
series 10: location:A20 R1 = 6 , R2 = 15 , TG = 195
series 11: location:A26 R1 = , R2 = , TG =
series 12: location:A32, R1 = 6 , R2 = 15, TG = TG high, use 195
series 13: location:A38, R1 = 6 , R2 = 15, TG = TG high, use 195

Comments:
Normal subject. She said that she did not move at all during scan. Should be a good study.

Fatsat seems working well in fgt1_new3d.

Date of study: 5/16a/98 study #: 4124
Breast Sequence Study
by David Zhu

Type of study: potato phantom(x )

Procedures:

1. 2D Spin Echo axial cut (Series 1) FOV = 40

2. David's breast sequence coronal cut: fgt1_new3d, fov = 34

Seven TI cycles: br_TR = 2.7 s, br_TI = 15 ms, ti_inc = 100 ms.
TI decreases from 615 ms to 15 ms.
Acquisitoin slice thickness: 3 mm, Selective slice thikness: 3mm
Frequency direction: R/L for all locations

(series 2)



Date of study: 5/16b/98 study #: 4123
Breast Sequence Study
by David Zhu

Meat phantom

Type of study:Meat phantom

Procedures:

1. 2D Spin Echo axial cut (Series 1) FOV = 40

2. David's breast sequence coronal cut: fgt1_new3d, fov = 34

Seven TI cycles: br_TR = 2.7 s, br_TI = 15 ms, ti_inc = 100 ms.
TI decreases from 615 ms to 15 ms.
Acquisitoin slice thickness: 3 mm, Selective slice thikness: 3mm
Frequency direction: R/L for all locations

(series 2)

3. David's breast sequence coronal cut: fgt1_new3d, fov = 34

Modified the following parameters to have: ti_inc = 10ms, br_TI = 550 ms

(series 3)

Purpose: To test the validity of motion correction algorithm when the the change of signal intensity is small.

Date of study: 5/16c/98 study #: 4126
Breast Sequence Study
by David Zhu

Type of study:potato phantom(x )

Procedures:

1. 2D Spin Echo axial cut (Series 1) FOV = 40

2. David's breast sequence coronal cut: fgt1_new3d, fov = 34

Seven TI cycles: br_TR = 2.7 s, br_TI = 15 ms, ti_inc = 100 ms.
TI decreases from 615 ms to 15 ms.
Acquisitoin slice thickness: 3 mm, Selective slice thikness: 3mm
Frequency direction: R/L for all locations

(series 2)

3. David's breast sequence coronal cut: fgt1_new3d, fov = 34

Modified the following parameters to have: ti_inc = 10ms, br_TI = 550 ms

(series 4)

Purpose: To test the validity of motion correction algorithm when the the change of signal intensity is small.

(Procedure Updated on 11/19/97)
Date of study: 4/13/98 study #: 3840
Breast Sequence Study
by Michael Buonocore and David Zhu

Type of study:phantom( ), normal subject ( ), subject w/ suspecious lesion (x)

Name: debra Age: about 40

Preparation:

Ask subject to have a better fit of the foam cast, tighter strap,
and not to move, and to breath smoothly with stomach.

Procedures:

1. 2D Spin Echo axial cut (Series 1)  FOV = 40  (named axial)

   I 84 to s 84 , loc:  . Scan thick = 5 mm, Inter = 1 mm.

2. 2D Fast Spin Echo (Series 2)  FOV = 34  (named highres)

   P 6 to A 96 , loc: 18 , scan thick = 5 mm, inter = 1 mm.

3. David's breast sequence coronal cut: fgt1_new3d, fov = 34

   Seven TI cycles: br_TR = 2.7 s, br_TI = 15 ms, ti_inc = 100 ms.
   TI decreases from 615 ms to 15 ms.
   Acquisitoin slice thickness: 3 mm,  Selective slice thikness: 3mm
   Frequency direction: R/L for all locations

| | | | |
|---|---|---|---|
| series 3: | location:A12 | R1 = 6 , R2 = 15 | , TG = 172 |
| series 4: | location: A18 | R1 = , R2 = | , TG = |
| series 5: | location: A24 | R1 = 6 , R2 = 15 | , TG = 172 |
| series 6: | location: A30 | R1 = , R2 = | , TG = |
| series 7: | location: A36 | R1 = 6 , R2 = 15 | , TG = 172 |
| series 8: | location: A42 | R1 = , R2 = | , TG = |
| series 9: | location: A48 | R1 = 6 , R2 = 15 | , TG = 173 |
| series 10: | location: A54 | R1 = , R2 = | , TG = |
| series 11: | location: A60 | R1 = 6 , R2 = 15 | , TG = 174 |
| series 12: | location: A66 | R1 = , R2 = | , TG = |
| series 13: | location: A72 | R1 = 6 , R2 = 15 | , TG = 175 |
| series 14: | location: A78 | R1 = , R2 = | , TG = |

Comments:
The suspicious mass is located at the right breast about two o'clock.

This subject later had a NEGATIVE biopsy result.

---

(Procedure Updated on 07/25/98)
Date of study: 7/27/98
Breast Sequence Study
by Michael Buonocore and David Zhu

Type of study:phantom( ), normal subject ( ), subject w/ suspecious lesion (x)

Name: Eileen D. Morrison Age: 64

Preparation:
Ask subject to have a better fit of the foam cast, tighter strap,
and not to move, and to breath smoothly with stomach.

Procedures:

1. 2D Spin Echo axial cut (Series 1 or axial)  FOV = 40

   I 84 to S 84 , loc: 29 . Scan thick = 5 mm, Inter =1 mm.

2. 2D Fast Spin Echo (Series 2 or highres)  FOV = 34

   P 10 to A 74 , loc: 15 , scan thick = 5 mm, inter = 1 mm.

3. SPGR dynamic contrast study (scan #1 in protocol): (series 3 -> dynamic)
   Each scan sequence takes total 30 sec with scan time 25 sec,
   and press time 5 sec.

   Note: The contrast study was not that successfully since the injection
   was not given successfully in terms of time.

   Scan sequences begin after about 2 minutes of injection.
   Total of 13 scan sequences with a total images of 169.



4. 3D scan (scan #2 in protocol, 2'37") with flip angle 20 degree. (series 4)
   28 slices with the center at A33.6.

5. David's breast sequence coronal cut: fgt1_new3d, fov = 34

   Seven TI cycles: br_TR = 2.7 s, br_TI = 15 ms, ti_inc = 100 ms.
   TI decreases from 615 ms to 15 ms.
   Acquisitoin slice thickness: 3 mm,  Selective slice thikness: 3mm
   Frequency direction: R/L for all locations

| | | | |
|---|---|---|---|
| series 5: | location: A8 | R1 = 6 , R2 = 15 | , TG = 183 |
| series 6: | location:A14 | R1 = , R2 = | , TG = |
| series 7: | location:A20 | R1 = 6 , R2 = 15 | , TG = 179 |
| series 8: | location:A26 | R1 = , R2 = | , TG = |
| series 9: | location:A32 | R1 = 6 , R2 = 15 | , TG = 182 |
| series 10: | location:A38 | R1 = 6 , R2 = 15 | , TG = 183 |
| series 11: | location:A44 | R1 = , R2 = | , TG = |

6. 3D scan (scan #2 in protocol, 2'37") with flip angle 65 degree.
   (series 12 -> post_3d)
   28 slices with the center at A33.6.

7. A phantom study to check the coil (series 13 )

Comments:
The contrast agent can last for hours.
The lesion is at the right side of the breast at about 9 o'clock.

Problems: (1) One side of the cable was broken and led to that the one side
did not receive the signal.
Replacing the cable with a feed-first cable would be ok. The coil is
fine.

(2) Contrast agent has not been performed correctly.

---

(Procedure Updated on 07/25/98)
Date of study: 8/7/98
Breast Study with Contrast
by Michael Buonocore and David Zhu

Type of study:phantom( ), normal subject ( ), subject w/ suspecious lesion (x)

Name: Marcie Drake  Age: 37  Weight: 135

Preparation:
Ask subject to have a better fit of the foam cast, tighter strap,
and not to move, and to breath smoothly with stomach.

Procedures:(Protocol: # 64)  (Study # 04817)

1. 2D Spin Echo axial cut (Series 1 -> axial)  FOV = 40

   I 84 to s 84 , loc: 29 . Scan thick = 5 mm, Inter = 1 mm.

2. 2D Fast Spin Echo (Series 2 -> highres)  FOV = 34

   P 10 to A 50 , loc:11 , scan thick = 5 mm, inter = 1 mm.

3. David's breast sequence coronal cut: fgt1_new3d, fov = 34

   Seven TI cycles: br_TR = 2.7 s, br_TI = 15 ms, ti_inc = 100 ms.
   TI decreases from 615 ms to 15 ms.
   Acquisitoin slice thickness: 3 mm,  Selective slice thikness: 3mm
   Frequency direction: R/L for all locations

| | | | |
|---|---|---|---|
| series 3: | location: P10 | R1 = 6 , R2 = 15 | , TG = 146 |
| series 4: | location: P4 | R1 = , R2 = | , TG = |
| series 5: | location: A2 | R1 = 6 , R2 = 15 | , TG = 150 |

series 6: location: A8 R1 = 6 , R2 = 15 , TG = 149
series 7: location: A14 R1 = , R2 = , TG =
series 8: location: A20 R1 = 6 , R2 = 15 , TG = 146
series 9: location: A26 R1 = , R2 = , TG =
series 10: location: A32 R1 = 6 , R2 = 15 , TG = 149
series 11: location: A38 R1 = , R2 = , TG =
series 12: location: A44 R1 = 6 , R2 = 15 , TG = 158
series 13: location: A50 R1 = 6 , R2 = 15 , TG = 151

4. Pre-contrast 3D scan (scan #2 in protocol, 2'37") (flip angle = 65)
(series 14 -> pre_3d_a)
(Center at A22.7 with 28 locs, 3 mm slice thickness)

5. More David's breast sequence coronal cut: fgt1_new3d, fov = 34

series 15: location: A23 R1 = 6 , R2 = 15 , TG = 145
series 16: location: A17 R1 = , R2 = , TG =
series 17: location: A29 R1 = 6 , R2 = 15 , TG = 148

---

The patient is pulled out to set up constrast injection in the following scans:

6. Pre-contrast 3D scan (scan #2 in protocol, 2'37") (flip angle = 65)
(series 18 -> pre_3d)
(repeat the pre_contrast) (Center at A22.7 with 28 locs, 3 mm slice thickness)

7. SPGR dynamic contrast study (total 7 minutes) (scan #1 in protocol):
(Series 19 -> dynamic)
Each scan sequence takes total 30 sec with scan time 25 sec,
with approximate interscan press time of 5 sec.

(1) 3 scan sequences before injection
(2) Begin injection and press SCAN to begin the 4th scan
(3) Continue on the same fashion to finish the 14th scan.

8. Post-contrast 3D scan (scan #2 in protocol, 2'37"), same as #6 above.
( Sereis 20 -> post_3d)
(Center at A22.7 with 28 locs, 3 mm slice thickness)

Comments:
Patient claims that the tumor locates at 10 o'clock in the right breast.
The patient has small breasts.
Foam packs have been adjusted to avoid motion
artifacts. Image displacement correction might need to consider.

Based on the analysis of the perfusion study, this patient appears
to be malignant in the right breast.

Biopsy indicated that the lesion(s) was benign.

DEPARTMENT OF THE ARMY
US ARMY MEDICAL RESEARCH AND MATERIEL COMMAND
504 SCOTT STREET
FORT DETRICK, MD 21702-5012

REPLY TO
ATTENTION OF

MCMR-RMI-S (70-1y) 1 July 03

MEMORANDUM FOR Administrator, Defense Technical Information Center (DTIC-OCA), 8725 John J. Kingman Road, Fort Belvoir, VA 22060-6218

SUBJECT: Request Change in Distribution Statement

1. The U.S. Army Medical Research and Materiel Command has reexamined the need for the limitation assigned to technical reports written for this Command. Request the limited distribution statement for the enclosed accession numbers be changed to "Approved for public release; distribution unlimited." These reports should be released to the National Technical Information Service.

2. Point of contact for this request is Ms. Kristin Morrow at DSN 343-7327 or by e-mail at Kristin.Morrow@det.amedd.army.mil.

FOR THE COMMANDER:

Encl

PHYLLIS M. RINEHART
Deputy Chief of Staff for
Information Management

ADB274518
ADB287328
ADB277943
ADB288221
ADB248332
ADB265760
ADB287619
ADB281577
ADB287600
ADB288422
ADB288375
ADB268297